Growing Schrödinger's cat states by local unitary time evolution of product states

Saverio Bocini ![ORCID] and Maurizio Fagotti ![ORCID]*

Université Paris-Saclay, CNRS, LPTMS, 91405 Orsay, France

We envisage many-body systems described by quantum spin-chain Hamiltonians featuring a trivial separable eigenstate. For generic Hamiltonians, such a state represents a quantum scar. We show that, typically, a macroscopically entangled state naturally grows after a single projective measurement of just one spin in the quantum scar. Moreover, we identify a condition under which what is growing is a "Schrödinger's cat state." Our analysis does not reveal any particular requirement for the entangled state to develop, provided that the quantum scar does not minimize/maximize a local conservation law. We study two explicit examples: systems described by generic Hamiltonians where spins interact in pairs, and models that exhibit a U(1) hidden symmetry. The latter can be reinterpreted as a two-leg ladder in which the interactions along the legs are controlled by the local state on the other leg through transistorlike building blocks.

Quantum superpositions of two macroscopically distinct states, known as "Schrödinger's cat states," from the famous Gedankenexperiment proposed by Schrödinger in 1935 [1,2], or also as "(generalized) GHZ states," from the observation by Greenberger, Horne, and Zeilinger [3] on quantum spin models escaping the original Bell's inequalities [4], are highly valuable due to their broad applications, e.g., in quantum metrology and quantum computation. They are, however, rare and generally short-lived because of their fragility under real experimental conditions, which include decoherence, noise, and particle loss. Several protocols have been proposed to overcome the latter problems [5–13], and some of them have been experimentally realized [14–17]. While such an instability undermines applications, it is, in fact, the defining feature of cat states, or, more generally, of states with extensive multipartite entanglement [18]. These are somehow unnatural states of matter in which fundamental physical properties such as cluster decomposition are lost. Engineering a cat state requires, therefore, a lot of control of the system, which, in turn, results in fine-tuned protocols designed with the clear goal of generating such exceptional states.

We propose a theoretical protocol to generate a cat state that stands out for its naturalness, in the sense that the growth of macroscopic entanglement is a manifestation of an intriguing physical phenomenon rather than of clever manipulations of a system. The most general system that we consider is described by a quantum spin-$\frac{1}{2}$ chain Hamiltonian $\mathbf{H}$ with local interactions and a trivial separable eigenstate. Without

---

*Contact author: maurizio.fagotti@universite-paris-saclay.fr

loss of generality, the latter can be set equal to

$$|\Psi(0)\rangle = |\Uparrow\rangle \equiv |\uparrow \cdots \uparrow\rangle, \tag{1}$$

where $|\uparrow\rangle$ denotes the eigenvector of the Pauli matrix σ^z with eigenvalue 1, and $\Uparrow$ will represent in this paper a generic number of adjacent $\uparrow$. Often the presence of such a trivial eigenstate is a consequence of a U(1) symmetry, e.g., the conservation of $\mathbf{S}^z = \frac{1}{2}\sum_\ell \boldsymbol{\sigma}_\ell^z$, where $\boldsymbol{\sigma}_\ell^\alpha$ are local operators acting like the Pauli matrices σ^α on site ℓ and like the identity elsewhere. As we will soon see, the most interesting cases are, however, those in which $\mathbf{S}^z$ is not conserved. If there are no additional relevant conserved operators, either $|\Uparrow\rangle$ is the ground state or it is an exact *quantum scar* [19–21]: its properties contrast with those of the eigenstates with similar energy. Quantum scars have recently attracted a lot of attention [21–23], also in connection with their unusual entanglement properties, displaying low bipartite entanglement, still potentially featuring extensive multipartite entanglement [24]. In our case the quantum scar is exceptional, as it is fully separable.

The basic idea is that the quantum scar is essentially metastable and could be transmuted into a state with extensive multipartite entanglement just by a local perturbation. Specifically, we consider the effect of a quantum measurement of a spin in a tilted direction with respect to z of an angle θ, so that the state is projected into

$$|\Psi_\theta(0^+)\rangle = e^{-i\theta\sigma_0^y}|\Uparrow\rangle = \cos\theta\,|\Uparrow\rangle + \sin\theta|\Uparrow\downarrow\Uparrow\rangle \tag{2}$$

with probability $\cos^2\theta$. Time evolution affects only the second term on the right-hand side of Eq. (2), hence

$$|\Psi_\theta(t)\rangle = \cos\theta\,|\Uparrow\rangle + \sin\theta e^{-i\mathbf{H}t}|\Uparrow\downarrow\Uparrow\rangle, \quad t > 0. \tag{3}$$

The Lieb-Robinson bounds [25] ensure that the perturbation is irrelevant outside a light cone emerging from the space-time point of the measurement. Since the state before the measurement is an eigenstate, the measurement triggers a
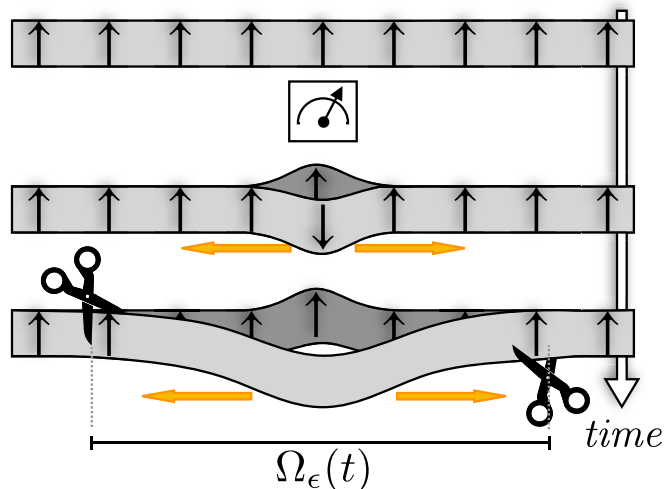
FIG. 1. Illustration of the protocol. The state with a single spin down time-evolves into a state that is macroscopically different from the premeasurement state. The scissors represent the fact that we ignore the region outside $\Omega_\epsilon(t)$.

nontrivial time evolution only within a region whose length grows linearly with time. Hence, neglecting the part of the system outside that region does not significantly affect the purity of the state. We call $\Omega_\epsilon(t)$ the smallest subsystem that contains the spin that is measured and that, as clarified later, can be considered pure at time t with accuracy $1 - \epsilon$. In the following, the use of terms such as "macroscopic" and "extensive" will refer to the subsystem $\Omega_\epsilon(t)$. This allows us to treat on the same footing infinite systems, which are arguably more interesting from a theoretical point of view, and finite ones [provided that the actual system size is larger than $\Omega_\epsilon(t)$], which are instead more relevant for the experiments. The situation is pictorially described in Fig. 1: after the spin flip at the origin, the component $|\Uparrow\downarrow\Uparrow\rangle$ of the state evolves in time, while the component $|\Uparrow\rangle$ stays constant; the effective size of the system is given by the spins that are inside the light cone originating from the local perturbation, while the rest of the spins are neglected.

First we show that, quite generally, in the settings considered the perturbation has everlasting effects on the expectation values of local observables arbitrarily far from the position of the measurement. That is to say, $e^{-i\mathbf{H}t}|\Uparrow\downarrow\Uparrow\rangle \equiv |\Psi_{\pi/2}(t)\rangle$ is macroscopically different from $|\Uparrow\rangle$, in that there exists an observable $\mathbf{A} = \sum_\ell \mathbf{a}_\ell$, with $\mathbf{a}_\ell$ operators with a finite support around site ℓ, such that $\langle\Uparrow|\mathbf{A}|\Uparrow\rangle - \langle\Psi_{\pi/2}(t)|\mathbf{A}|\Psi_{\pi/2}(t)\rangle$ is extensive, i.e., it scales linearly with the (effective) system size $|\Omega_\epsilon(t)|$ [26]. Such an effect is already remarkable, as, generally, local perturbations in quantum many-body systems either fade away or remain localized.

We then delve into extensive entanglement, noting that a pure state is said to possess extensive multipartite entanglement if and only if the variance scales as the square of the system size for at least one extensive operator [27–29]. Because $|\Psi_{\pi/2}(t)\rangle$ is macroscopically different from $|\Uparrow\rangle$, the reader is already in the position to infer that the projective measurement on the quantum scar $|\Uparrow\rangle$ will likely generate a state with extensive multipartite entanglement. This inference

is supported by the fact that, if the extensive operator $\mathbf{A}$ can take values in $|\Psi_\theta(t)\rangle$ separated by $O(|\Omega_\epsilon(t)|)$ with significant probability, its variance in the state will be $O(|\Omega_\epsilon(t)|^2)$, directly implying macroscopic entanglement. But the situation is even more interesting. We provide evidence and then conjecture that, if the model has a hidden U(1) symmetry (see below for the definition), $|\Psi_{\pi/2}(t)\rangle$ is not macroscopically entangled; under those conditions, the projective measurement generates a genuine Schrödinger's cat state consisting of an (ideally) arbitrarily large number of sites.

I. SYSTEMS UNDER CONSIDERATION

We are going to investigate a variety of Hamiltonians with local densities. Our requirement of $|\Uparrow\rangle$ being an eigenstate of the Hamiltonian allows for any kinds of interactions that commute with the total spin in the z direction, $\mathbf{S}^z = \frac{1}{2}\sum_\ell \boldsymbol{\sigma}_\ell^z$ (such as the hopping term $\boldsymbol{\sigma}_\ell^x\boldsymbol{\sigma}_{\ell+n}^x + \boldsymbol{\sigma}_\ell^y\boldsymbol{\sigma}_{\ell+n}^y$ or the longitudinal Dzyaloshinskii-Moriya interaction $\boldsymbol{\sigma}_\ell^x\boldsymbol{\sigma}_{\ell+n}^y - \boldsymbol{\sigma}_\ell^y\boldsymbol{\sigma}_{\ell+n}^x$), but not only that. The constraint is much weaker than U(1) symmetry, and the Hamiltonian density can feature any term of the form $\frac{1-\boldsymbol{\sigma}_\ell^z}{2}\mathbf{O}_\ell\frac{1-\boldsymbol{\sigma}_\ell^z}{2}$, where $\mathbf{O}_\ell$ is a local operator with support in a region around ℓ.

We start by discussing the general form of the Hamiltonians under consideration, categorizing them into two groups based on the presence or absence of a *hidden* U(1) symmetry.

A. Systems with hidden U(1) symmetry

The first class of Hamiltonians we consider has recently sparked some attention because it describes systems that are macroscopically sensitive to local perturbations [30,31]. Such a sensitivity is triggered by so-called "semilocal conservation laws," whose densities act as local observables only in a restricted space characterized by a particular symmetry. This unusual property could seem innocuous at first glance, but it allows the state to retain a memory of so-called "string order" [32–34], thus enabling symmetry-protected topological order to survive the limit of infinite time [31]. An example of an operator with a semilocal density in a system that is symmetric under the spin flip $\boldsymbol{\sigma}_\ell^{x,y} \to -\boldsymbol{\sigma}_\ell^{x,y}$ is

$$\tilde{\mathbf{S}}^z = \frac{1}{2}\sum_\ell \mathbf{\Pi}^z(\ell), \qquad (4)$$

where $\mathbf{\Pi}^z(\ell)$ can be thought of as a semi-infinite string of $\boldsymbol{\sigma}_\ell^z$ and is such that $[\mathbf{\Pi}^z(\ell)]^2 = \mathbf{I}$, $[\mathbf{\Pi}^z(\ell), \boldsymbol{\sigma}_j^z] = 0$, and $\mathbf{\Pi}^z(\ell)\boldsymbol{\sigma}_j^{x,y} = \text{sgn}(\ell - j - \frac{1}{2})\boldsymbol{\sigma}_j^{x,y}\mathbf{\Pi}^z(\ell)$. In spin-flip invariant settings, the density $\mathbf{\Pi}^z(\ell)$ of $\tilde{\mathbf{S}}^z$ is a local observable, and, if $\tilde{\mathbf{S}}^z$ commutes with the Hamiltonian, it has important consequences on the evolution of the system, similarly to any other local conservation law—we refer the reader to Ref. [31] for additional details.

The behavior of fluctuations in these systems has not yet been investigated, but the sensitivity of local observables to a single spin flip is a strong indication that the quantum measurement of a local observable such as $\boldsymbol{\sigma}_j^x$ could result in macroscopically entangled states. As a specific example, we
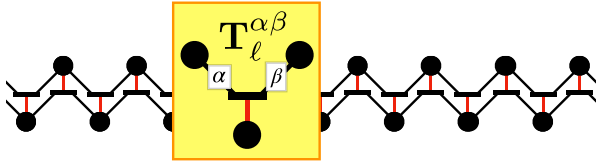
FIG. 2. Pictorial representation of the quantum transistor chain, constructed as a sequence of building blocks $\mathbf{T}_\ell^{\alpha\beta} = \boldsymbol{\sigma}_{\ell-1}^\alpha \frac{\mathbf{I}-\sigma_\ell^z}{2} \boldsymbol{\sigma}_{\ell+1}^\beta$.

consider the following Hamiltonian:

$$\mathbf{H}_1 = \sum_\ell \frac{\mathbf{1}-\boldsymbol{\sigma}_\ell^z}{8} \left[J\vec{\boldsymbol{\sigma}}_{\ell-1} \overset{S}{\cdot} \vec{\boldsymbol{\sigma}}_{\ell+1} + \vec{D} \cdot (\vec{\boldsymbol{\sigma}}_{\ell-1} \times \vec{\boldsymbol{\sigma}}_{\ell+1}) \right]$$
$$- \frac{\vec{h}}{2} \cdot \vec{\boldsymbol{\sigma}}_\ell, \tag{5}$$

where $\vec{a} \overset{S}{\cdot} \vec{b} \equiv \vec{a} \cdot (S\vec{b})$. This Hamiltonian commutes with the semilocal charge $\tilde{\mathbf{S}}^z$—Eq. (4)—provided that

$$S = \begin{bmatrix} \frac{1+\gamma}{2} & w & 0 \\ w & \frac{1-\gamma}{2} & 0 \\ 0 & 0 & \Delta \end{bmatrix}, \quad \vec{D} = \begin{bmatrix} 0 \\ 0 \\ D^z \end{bmatrix}, \quad \vec{h} = \begin{bmatrix} 0 \\ 0 \\ h^z \end{bmatrix}. \tag{6}$$

It describes a system that can be interpreted as a quantum transistor chain, in which the building blocks $\mathbf{T}_\ell^{\alpha\beta} = \boldsymbol{\sigma}_{\ell-1}^\alpha \frac{\mathbf{I}-\sigma_\ell^z}{2} \boldsymbol{\sigma}_{\ell+1}^\beta$, with $(\alpha, \beta) \in \{(x,x), (x,y), (y,x), (y,y), (z,z), (0,0)\}$ ($\sigma_\ell^0 \equiv \mathbf{1}$), commute with $\tilde{\mathbf{S}}^z$—see Fig. 2. This transistorlike configuration offers an insightful interpretation of time evolution, as elaborated on in Sec. III B.

It is known that $\mathbf{H}_1$ has infinitely many conserved operators with quasilocal [35] or semilocal [31] densities in the following regions of the parameter space:

(i) If the only nonzero coupling constants are J, γ, and h^z, and $\gamma = \pm 1$, the model is dual to the (integrable) Heisenberg *XXZ* one [30,36].

(ii) If the only nonzero coupling constants are J, Δ, and h^z, the model belongs to the family of hard-rod deformations of *XXZ* studied in Ref. [37]. In particular, for $\Delta = 0$ it is a special case of the Bariev model [38] and was recently dubbed *dual folded XXZ* [36]. These are special integrable models exhibiting Hilbert-space fragmentation and quantum jamming [36,39–41].

In all the other instances that we have considered, to rule integrability out, we have verified that the statistics of the energy levels is in agreement with a Wigner-Dyson distribution (see Appendix A).

For the first family of integrable models, Ref. [30] has already shown that $|\Psi_{\pi/2}(t)\rangle$ and $|\Uparrow\rangle$ become macroscopically different in time. An analogous conclusion was drawn in Refs. [40,41] for the second family of integrable models, though starting from slightly different product states [in those systems, $|\Uparrow\downarrow\Uparrow\rangle$ is an eigenstate as well, leading to $|\psi_\theta(t)\rangle = |\psi_\theta(0)\rangle$, $\forall\theta$]. Reference [40] also observed that a similar behavior could be seen even in generic systems with a jamming sector. We announce that a part of the phenomenology common to all these settings is much more general than the specific models studied so far.

B. Generic systems

We establish contact with the systems currently studied in quantum simulators, for example with trapped ions [42], by considering the following Hamiltonian:

$$\mathbf{H}_2 = \frac{1}{4} \sum_\ell \left[\sum_{r=1} J_r \vec{\boldsymbol{\sigma}}_\ell \overset{S_r}{\cdot} \vec{\boldsymbol{\sigma}}_{\ell+r} + \vec{D}_r \cdot (\vec{\boldsymbol{\sigma}}_\ell \times \vec{\boldsymbol{\sigma}}_{\ell+r}) \right] - \frac{\vec{h}}{2} \cdot \vec{\boldsymbol{\sigma}}_\ell. \tag{7}$$

This is the most general Hamiltonian where spins interact in pairs: there is a Heisenberg exchange term, a Dzyaloshinskii-Moriya interaction, and a coupling with an external field. The trivial quantum scar $|\Uparrow\rangle$ appears when

$$S_r = \begin{bmatrix} 1 & 0 & \frac{1}{2}\gamma_r^x \\ 0 & 1 & \frac{1}{2}\gamma_r^y \\ \frac{1}{2}\gamma_r^x & \frac{1}{2}\gamma_r^y & 1+\gamma_r^z \end{bmatrix}, \quad \vec{h} = \begin{bmatrix} \frac{1}{2}\sum_{r=1} J_r\gamma_r^x \\ \frac{1}{2}\sum_{r=1} J_r\gamma_r^y \\ h^z \end{bmatrix}. \tag{8}$$

The parameter $\vec{\gamma}$ incorporates both an anisotropy in the Heisenberg interaction and a rotation of the axes (which is relevant because we have fixed the orientation of the spins of the separable eigenstate). As will be clarified soon, the effect we exploit to generate macroscopically entangled states requires a U(1)-breaking interaction, therefore we will only consider systems in which some coupling constants among $D_r^x, D_r^y, \gamma_r^x, \gamma_r^y$ are nonzero.

In such a generic setting, there is no *a priori* reason to expect the localized perturbation to produce macroscopic effects; for example, the system does not exhibit semilocal charges or special constraining interactions. Is the presence of a simple quantum scar sufficient to trigger the phenomenon?

Before reporting the results of our investigation, we remind the reader of some special regions of the parameter space:

(i) If the only nonzero coupling constants are J_1, γ_1^z, and h^z, the system is integrable and known as the *XXZ model*, which is arguably the most important paradigm of quantum magnetism in 1D [43].[1]

(ii) More generally, if $\vec{D}_r = 0$ and $\vec{\gamma}_r = \vec{\gamma}_1$, the system describes an *XYZ* Heisenberg model with a tilted orientation, the integrable case corresponding to $\vec{h} = 0$ and $J_r = \delta_{r,1}J_1$. See also Ref. [44] for a special region of the parameter space in which $|\Uparrow\rangle$ becomes the symmetry-breaking ground state.

(iii) If the only nonzero coupling constants are J_1, γ_1^x, D_1^y, and h^z, in the limit $J_1 \to 0$ at fixed $\gamma_1^x J_1 = -2D_1^y$ the system approaches the so-called quantum East model [45], which has recently attracted a lot of attention for its unusual properties [46].

II. FRAMEWORK AND ESSENTIAL DEFINITIONS

In this section we elaborate on some key concepts brought up in the Introduction, including the notion of effective subsystem $\Omega_\epsilon(t)$, as well as macroscopic entanglement and cat states.

---

[1]Sometimes, especially in experimental works, the name *XXZ model* is used to refer to a broader range of models, including those with nonzero J_r and γ_r for any r, provided that $\gamma_r^z = \gamma_1^z$.

A. The effective system $\Omega(t)$

We have introduced $\Omega_\epsilon(t)$ as the smallest subsystem containing the measured spin that can be considered pure at time t with accuracy $1 - \epsilon$. We clarify this point here. First of all, it can be readily proven that the initial perturbation is irrelevant outside a light cone emerging from the space-time point of the measurement using a corollary of the Lieb-Robinson bounds derived in Ref. [47]. Indeed, the Heisenberg representation of a local operator is exponentially close to an operator with support in a finite region including the support of the operator, the argument of the exponential being proportional to $d - v_{LR}|t|$, where d is the smallest distance between the observable and the boundary of the region, and v_{LR} is the Lieb-Robinson velocity. In our specific case, this means that the following decomposition holds: $\exp[i\theta\boldsymbol{\sigma}_0^y(-t)] = \mathbf{U}_\Omega + \boldsymbol{\Delta}_\Omega$, where $\mathbf{U}_\Omega$ is a unitary operator with support in a region Ω centered at the measurement position and $\|\boldsymbol{\Delta}_\Omega\| \lesssim \exp[-(|\Omega|/2 - vt)/\xi]$, with ξ a nonuniversal constant. This gives

$$\| |\Psi(t)\rangle \langle\Psi(t)| - \mathbf{U}_\Omega |\Uparrow\rangle \langle\Uparrow| \mathbf{U}_\Omega^\dagger \|$$

$$= \|\mathbf{U}_\Omega |\Uparrow\rangle \langle\Uparrow| \boldsymbol{\Delta}_\Omega^\dagger + \boldsymbol{\Delta}_\Omega |\Uparrow\rangle \langle\Uparrow| \mathbf{U}_\Omega + \boldsymbol{\Delta}_\Omega |\Uparrow\rangle \langle\Uparrow| \boldsymbol{\Delta}_\Omega^\dagger \|$$

$$\leqslant 2\|\boldsymbol{\Delta}_\Omega\| + \|\boldsymbol{\Delta}_\Omega\|^2 \lesssim e^{-(|\Omega|/2 - vt)}, \qquad (9)$$

that is to say, up to exponentially small corrections the reduced density matrix of Ω is pure.

We call $\Omega_\epsilon(t)$ the smallest spin block for which

$$\|\text{tr}_{\overline{\Omega_\epsilon(t)}}[e^{-i\mathbf{H}t}|\Uparrow\downarrow\Uparrow\rangle\langle\Uparrow\downarrow\Uparrow|e^{i\mathbf{H}t}] - (|\Uparrow\rangle\langle\Uparrow|)_{\overline{\Omega_\epsilon(t)}}\| \leqslant \epsilon, \quad (10)$$

where $(|\Uparrow\rangle\langle\Uparrow|)_{\overline{\Omega_\epsilon(t)}}$ is the state $|\Uparrow\rangle$ restricted to the complement of $\Omega_\epsilon(t)$. Note that $\Omega_\epsilon(0)$ contains only the spin at the origin for any choice of ϵ.

B. Macroscopic entanglement and cat states

We measure macroscopic entanglement with the so called *quantumness*, which characterizes the asymptotic behavior of the maximum quantum Fisher information among all extensive observables. A quantumness that grows linearly with system size defines a macroscopically entangled state [29]. In fact, as is typically done [26], we only compute a lower bound of it, $N_{\text{eff}}^{(1)}$, resulting from reducing the space of observables. We refer the reader to Sec. V C for a more extended discussion about the quantumness.

A cat state is a special state with macroscopic entanglement. What characterizes it is that it can be expressed as the linear superposition of two states, each of which does not possess macroscopic entanglement. The archetypal example of a cat state is the GHZ state $(|\Uparrow\rangle + |\Downarrow\rangle)/\sqrt{2}$.

III. RESULTS

In this section, we explore macroscopic entanglement and cat state formation within the framework of our proposed protocol. First, we discuss how U(1) symmetry would inhibit the growth of macroscopic entanglement. Next, we show the main results for systems without U(1) symmetry. Finally, we provide a study of the robustness of the protocol, showing that macroscopic entanglement survives small modifications of the initial state. However, perturbations that break spin-flip symmetry hinder the formation of a cat state.

A. U(1) hinders macroscopic entanglement

If the total magnetization $\mathbf{S}^z$ is conserved, the states $|\Uparrow\rangle$ and $|\Psi_{\pi/2}(t)\rangle$ cannot be macroscopically different for any time t, and therefore their linear combination is not macroscopically entangled. Specifically, Appendix D provides a proof that the quantity $\langle\Psi|\mathbf{O}|\Psi\rangle - \langle\Uparrow|\mathbf{O}|\Uparrow\rangle$ is subextensive for any operator $\mathbf{O} = \sum_\ell \mathbf{O}_\ell$, where $\mathbf{O}_\ell$ are local operators with support in a finite subsystem around site ℓ. This is equivalent to saying that a state $|\Psi\rangle$ obtained by time evolution under a U(1)-symmetric Hamiltonian after a local perturbation to $|\Uparrow\rangle$ is macroscopically equivalent to $|\Uparrow\rangle$. Appendix D also proves that the variance of any of such operators $\mathbf{O}$ with respect to the state $|\Psi\rangle$ grows at most linearly with the (effective) system size $|\Omega_\epsilon(t)|$, ruling out the possibility to obtain a macroscopically entangled state from the time evolution of a locally perturbed $|\Uparrow\rangle$. And this holds true for any local perturbation. Physically, we can understand this result from the fact that, first, a local operator can only flip a finite number of spins, and second, the initial state, $|\Uparrow\rangle$, has maximal $\mathbf{S}^z$. As a result, the Hilbert space accessible to time evolution is too small for macroscopic entanglement to develop. This is the first clue supporting the expectation that, in order to build up macroscopic entanglement, $|\Uparrow\rangle$ cannot be the ground state of a local conservation law. In generic systems, we can read this as a statement that $|\Uparrow\rangle$ should be a quantum scar.

B. Hidden U(1) leads to a cat state

We start with $\mathbf{H}_1$—Eq. (5)—in the integrability region in which, as discussed in Sec. I A, we can take for granted that $|\Psi_{\pi/2}(t)\rangle$ becomes macroscopically different from $|\Uparrow\rangle$. In particular, we can assume

$$|\langle\Uparrow\downarrow\Uparrow|e^{i\mathbf{H}_1 t}\mathbf{S}^z e^{-i\mathbf{H}_1 t}|\Uparrow\downarrow\Uparrow\rangle - \langle\Uparrow|\mathbf{S}^z|\Uparrow\rangle| \sim t, \qquad (11)$$

as long as the initial state $|\Uparrow\rangle$ is in the middle of the spectrum of $\mathbf{H}_1$. The importance of the latter condition is discussed in Sec. IV B. Figure 3(a) shows how the difference of magnetization between flipping or not flipping the spin is proportional to $|\Omega_\epsilon(t)| \sim t$, meaning that the two states $|\Uparrow\rangle$ and $|\Psi_{\pi/2}(t)\rangle$ are macroscopically different. Note also that from the profile of the local magnetization [inset of Fig. 3(a)] we get a visual definition of $\Omega_\epsilon(t)$: it essentially coincides with the region with $\langle\boldsymbol{\sigma}_\ell^z(t)\rangle \not\approx 1$ and, because the profile is constant in the ballistic scale, we see that $|\Omega_\epsilon(t)|$ grows linearly in system size.

In the integrability region of $\mathbf{H}_1$ there is just one piece of information that we cannot retrieve from the scientific literature: the behavior of fluctuations of extensive observables in the state $|\Psi\rangle$ resulting from time evolution. We address this gap by studying the quantumness of $|\Psi_\theta(t)\rangle$. An example of the results that we get is reported in Fig. 3(b), where we plot the quantumness $N_{\text{eff}}^{(1)}$ as a function of the effective system size $|\Omega_\epsilon(t)|$.[2] To study the asymptotic behavior of $N_{\text{eff}}^{(1)}$, we fit the

---

[2]The quantumness is reported as a function of $|\Omega_\epsilon(t)|$ (and not t) because one looks at the scaling of the quantumness with respect to system size to characterize macroscopic entanglement [29]. Note, however, that, since $|\Omega_\epsilon(t)|$ grows linearly in time (cf. Appendix B), the plot would be qualitatively the same if we replace $|\Omega_\epsilon(t)|$ with t.
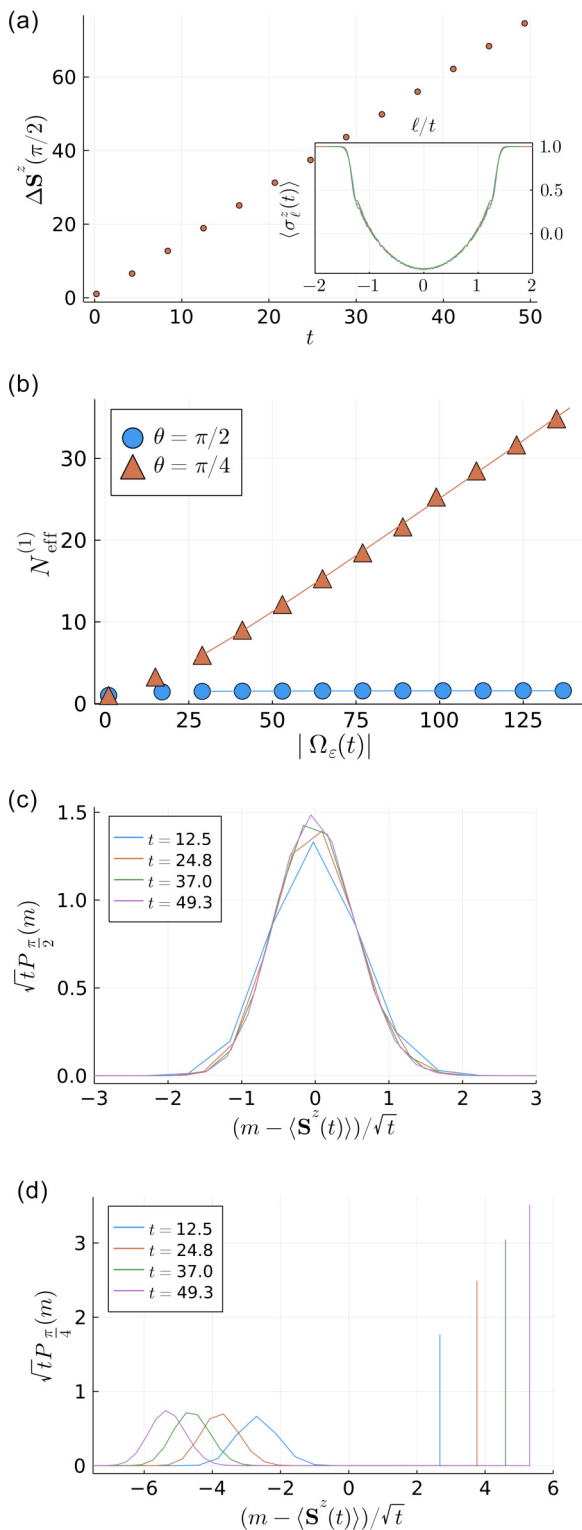
FIG. 3. Time evolution of $|\Psi_\theta(t)\rangle$ under Hamiltonian $\mathbf{H} = J \sum_\ell \frac{1-\sigma_\ell^z}{2} \sigma_{\ell-1}^x \sigma_{\ell+1}^x$, with $J = 2.8$, which is an integrable point of the Hamiltonian $\mathbf{H}_1$ with hidden $U(1)$ symmetry. (a) Difference between the total magnetization in $|\Uparrow\rangle$ and $|\Psi_{\pi/2}(t)\rangle$, i.e. $\Delta \mathbf{S}^z(\theta) = \langle\Uparrow |\mathbf{S}^z|\Uparrow\rangle - \langle\Psi_\theta(t)|\mathbf{S}^z|\Psi_\theta(t)\rangle$; inset: local magnetization profile for the last four times of the main plot. (b) Macroscopic quantumness as a function of the effective system size $|\Omega_\varepsilon(t)|$, with $\epsilon = 0.001$. (c) and (d) Probability distribution $P_\theta(m)$ for $\theta = \frac{\pi}{2}$ and $\theta = \frac{\pi}{4}$, respectively.

data with a curve parametrized as $\beta_0 + \beta_1|\Omega_\epsilon(t)| + \beta_2 \frac{1}{|\Omega_\epsilon(t)|}$, where the term $\frac{1}{|\Omega_\epsilon(t)|}$ stands for a potential subleading term. The estimated leading order is consistent with a constant ($\beta_1 \approx 0$) in the case $\theta = \pi/2$ and with a linear growth ($\beta_1 \neq 0$) in the generic case.

To gain another perspective on the entanglement properties of the state, we also look at the probability distribution $P_\theta(m)$ to get m from a measurement of $\mathbf{S}^z$ given that the system is in the state $|\Psi_\theta(t)\rangle$. Note that, by its definition, a cat state is characterized by a bimodal distribution with well-separated peaks; consider, e.g., the GHZ state $(|\Uparrow\rangle + |\Downarrow\rangle)/\sqrt{2}$, where the probability distribution exhibits two Kronecker δ's at the maximum and minimum magnetizations. For the state $\theta = \frac{\pi}{2}$, the probability distribution shows standard fluctuations [Fig. 3(c)], with a variance scaling as the effective system size. In contrast, for $\theta \notin \{0, \frac{\pi}{2}\}$, we get the bimodal distribution that is characteristic of a cat state [Fig. 3(d)]. Comparing the latter with the GHZ case, we see that one δ is replaced by a Gaussian centered at a different magnetization, but it is still well separated from the other peak. Note that in the figure, we have shifted m by the expectation value of $\mathbf{S}^z(t)$ to exhibit plots independent of the system size. Incidentally, this also allows us to consider either the full chain or $\Omega_\epsilon(t)$ equivalently.

As we move away from the integrability region of $\mathbf{H}_1$, we have verified that, provided the initial state resides within the bulk of the spectrum, the qualitative behavior remains consistent even beyond that region. An example is reported in Fig. 4. Remarkably, even in this nonintegrable case, the profiles of local magnetization (the insets in the plots of the total magnetization) computed at different times collapse to the same curve in the ray coordinate ℓ/t, which manifests the ballistic change in the total magnetization.

We mention that the tidy structure of the transistor Hamiltonian $\mathbf{H}_1$ allows for an insightful interpretation of the protocol. The state before the measurement has all transistor *switches* open, and time evolution is blocked. The measurement has the effect of turning a switch in a quantum superposition of open and closed (the switch is exactly closed only for $\theta = \frac{\pi}{2}$). Closing a switch enables Heisenberg and Dzyaloshinskii-Moriya interactions between the neighboring spins of the opposite leg of the chain, which, in turn, partially close other switches, and so on and so forth, leading to a complete reconfiguration of the state that affects a region whose size grows linearly in time.

C. General growth of macroscopic entanglement

We have considered several models without a hidden $U(1)$ symmetry in which $|\Uparrow\rangle$ is still a quantum scar. We see quite generally that, also in those cases, the spin flip has everlasting effects arbitrarily far from the origin. In Fig. 5 we report an example using the Hamiltonian $\mathbf{H}_2$—Eq. (7). The plot of the magnetization shows that the states $|\Uparrow\rangle$ and $|\Psi_{\pi/2}(t)\rangle$ are macroscopically different: the difference of the magnetization in the two states grows linearly with the effective system size. Concerning the quantumness, we have fitted the data for the lower bound $N_{\text{eff}}^{(1)}$ with the same ansatz as before, $\beta_0 + \beta_1|\Omega_\epsilon(t)| + \beta_2 \frac{1}{|\Omega_\epsilon(t)|}$; the analysis points to an asymptotic linear growth for any $\theta \neq 0$, including this time also
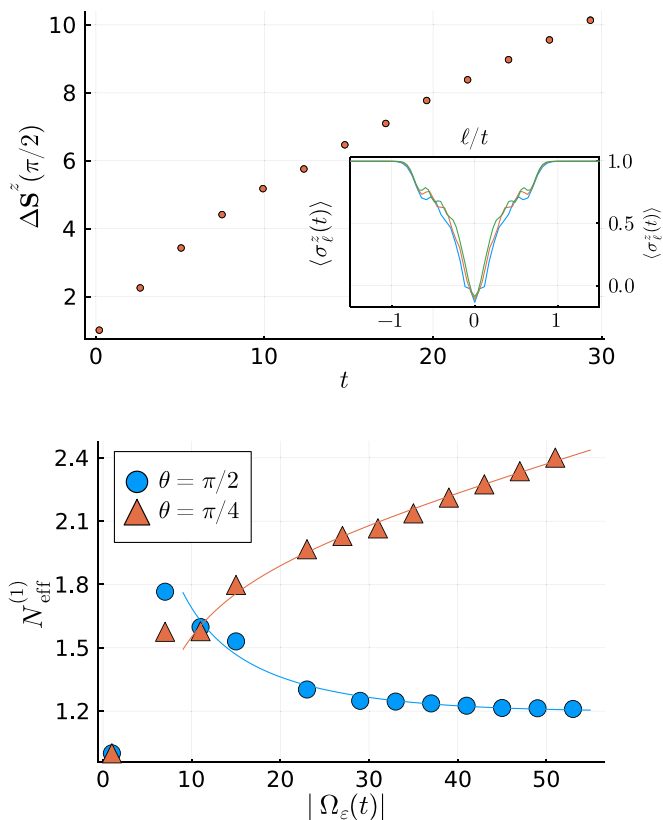
FIG. 4. The same as in the top plots of Fig. 3 for Hamiltonian $\mathbf{H} = \sum_\ell \frac{1-\sigma_\ell^z}{8}(\frac{3}{2}\sigma_{\ell-1}^x\sigma_{\ell+1}^x + \frac{1}{2}\sigma_{\ell-1}^y\sigma_{\ell+1}^y + J_{xy}\sigma_{\ell-1}^x\sigma_{\ell+1}^y + J_{yx}\sigma_{\ell-1}^y\sigma_{\ell+1}^x)$, $J_{xy} = 1.3$, $J_{yx} = 0.1$, which is a nonintegrable point of the Hamiltonian $\mathbf{H}_1$ with hidden U(1) symmetry.

$\theta = \frac{\pi}{2}$. Therefore, $|\Psi_\theta(t)\rangle$ still exhibits macroscopic entanglement for generic θ, but, in contrast to the quantum transistor chain, also $|\Psi_{\pi/2}(t)\rangle$ is macroscopically entangled, undermining in turn the formation of a cat state.

D. Imperfections in the preparation of the state

We investigate the effect of perturbing the state $|\Uparrow\rangle$ before performing the local measurement. For simplicity, we restrict to perturbations that consist in time evolving $|\Uparrow\rangle$ under a homogeneous Hamiltonian $\mathbf{H}_0$ for a fixed time t_0, in such a way that the state before the local measurement is $|\Psi_0(0^-)\rangle = e^{-i\mathbf{H}_0 t_0}|\Uparrow\rangle$. We then study the time evolution of $|\Psi_\theta(0^+)\rangle = e^{i\theta\sigma_0^y}|\Psi_0(0^-)\rangle$, which is the analog of Eq. (2). We warn the reader of a complication: the initial evolution affects the whole chain, so, strictly speaking, there is no approximately pure subsystem $\Omega_\epsilon(t)$. If we insist on considering the subsystem associated with the spreading of the local perturbation (corresponding to the sharp change of behavior in the profile of the magnetization), we should analyze the quantum Fisher information of a mixed state, which is a harder quantity to compute. In this preliminary study of the stability of our protocol, we limit ourselves to checking the qualitative behavior of the probability distribution of the magnetization.

We distinguish two classes of perturbations: in the first class, the perturbation is spin-flip symmetric [thus the hidden U(1) symmetry is preserved], e.g., $\mathbf{H}_0$ could be the integrable
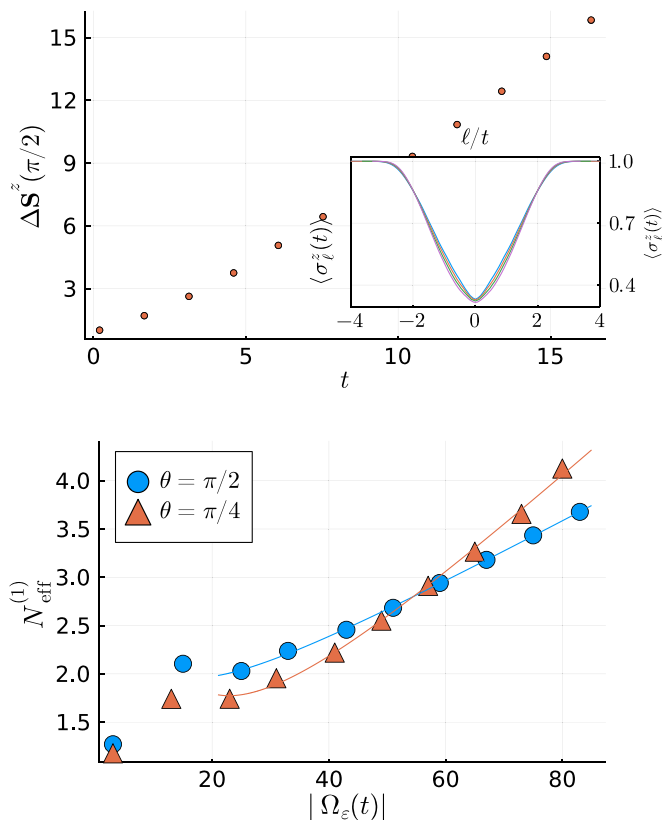

FIG. 5. The same as in the top plots of Fig. 3 for Hamiltonian $\mathbf{H} = \frac{1}{4}\sum_\ell[\sigma_\ell^x\sigma_{\ell+1}^x + \sigma_\ell^y\sigma_{\ell+1}^y + \sigma_\ell^x\sigma_{\ell+2}^x + \sigma_\ell^y\sigma_{\ell+2}^y + \Delta(\sigma_\ell^z\sigma_{\ell+1}^z + \sigma_\ell^z\sigma_{\ell+2}^z) + D(\sigma_\ell^x\sigma_{\ell+1}^z - \sigma_\ell^z\sigma_{\ell+1}^x)]$, $\Delta = 0.4$, $D = 0.9$, which is a nonintegrable point of Hamiltonian $\mathbf{H}_2$ without hidden U(1) symmetry. The widest profile in the inset corresponds to the largest time.

Ising Hamiltonian

$$\mathbf{H}_{0,1} = -\frac{1}{4}\sum_\ell\left(\sigma_\ell^x\sigma_{\ell+1}^x + h_0^z\sigma_\ell^z\right); \tag{12}$$

in the second class, the premeasurement Hamiltonian breaks the spin-flip invariance behind the hidden U(1) symmetry, e.g.,

$$\mathbf{H}_{0,2} = -\frac{1}{4}\sum_\ell\left(\sigma_\ell^x\sigma_{\ell+1}^x + h_0^z\sigma_\ell^z + h_0^x\sigma_\ell^x\right), \tag{13}$$

which is a nonintegrable version of the Ising model. Note that, in both cases, the larger h_0^z is, the smaller is the expected effect, therefore h_0^z can be used as a control parameter.

The first class of perturbations is not expected to destabilize the growth of a cat state: On the one hand, Ref. [30] showed that the perturbation has everlasting macroscopic effects even after so-called "global quenches" from a spin-flip invariant initial state. On the other hand, Ref. [48] indirectly confirms clustering in $|\Psi_{\pi/2}(t)\rangle$ at long times with noninteracting transistor Hamiltonians by showing that the mutual information approaches zero at large distances. Our numerical analysis is consistent with these expectations. Indeed, we still see the formation of a bimodal probability distribution (with two well-separated peaks).
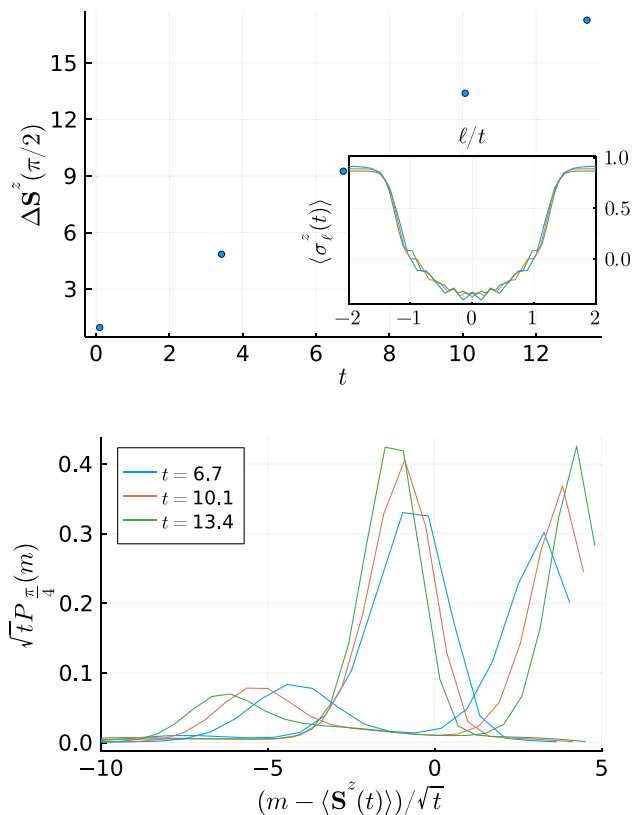
FIG. 6. Time evolution under $\mathbf{H}_1$ after perturbing the state $|\Uparrow\rangle$ with $\mathbf{H}_{0,2}$ for a time $t_0 = 0.4$. The parameters are set to $J = 2.8$, $\gamma = 1$, $w = \Delta = D^z = h^z = 0$ for $\mathbf{H}_1$; and $h_0^z = 0.7$ and $h_0^x = 0.5$ for $\mathbf{H}_{0,2}$. Top: the difference in magnetization with or without the spin flip grows linearly in time, at least for the times reached by our simulation; inset: local magnetization profile for the last four times of the main plot. Bottom: more than two peaks appear and they are not well-separated.

IV. DISCUSSION

In this section, we contextualize our findings within the broader framework of quantum quenches, emphasizing the exceptional nature of the phenomenon we discussed.

A. Local perturbations with macroscopic effects

In ordinary 1D systems, a spin flip does not change the macroscopic properties of a state regardless of how long the time is. The naive expectation is that its effect spreads out across the chain as t^α but fades away as $t^{-\alpha}$, with $\alpha = 1$ in integrable models and $\alpha = \frac{1}{2}$ in most of the generic systems. Recently, three situations have been pointed out in which this picture can break down:

(i) Ground states in symmetry-broken phases [49,50].

(ii) Quantum jammed states in systems with Hilbert space fragmentation [40].

(iii) Systems with semilocal conservation laws [30].

To these three known cases, we have added models with a fully separable quantum scar. This novel scenario has two advantages: first, a product state can be easily prepared experimentally, and second, its stationarity ensures that the (virtual) experiment can stop at any time without compromising the outcome.

Remarkably, the norm is that the perturbation generates macroscopic entanglement. Moreover, in the special case in which there is hidden U(1) symmetry, our analysis of the fluctuations reveals that the entangled part of the system is in a Schrödinger's cat state.

B. On the spreading

The existence of the semilocal charge $\sum_\ell \mathbf{\Pi}^z(\ell)$ ensures that the effect of the spin flip does not fade away over long timescales [30,31]. However, it alone is insufficient to prevent the effect from remaining localized around the measurement position (see Appendix C). An illustrative example of this behavior is provided by the Hamiltonian $\mathbf{H}_1$—Eq. (5)—in the parameter regime dubbed *dual XXZ model*. Here, for $|h^z|$ large enough, $|\Uparrow\rangle$ becomes the ground state (or the maximum energy state). By applying the Kramers-Wannier duality mapping proposed in Ref. [30], the system is mapped into the time evolution of a domain wall in the *XXZ* model, where the magnetic field h^z plays the role of the anisotropy. As proven in Ref. [51], the domain wall does not spread when the anisotropy is larger than a critical value, which is equivalent to saying that the perturbation remains localized when $|h^z|$ is large enough to move $|\Uparrow\rangle$ at the boundaries of the energy spectrum.

In the generic case, however, the perturbation spreads out. Using the underlying integrable structure, Ref. [30] showed that the spreading is ballistic for $\gamma = 1$, $w = \Delta = D^z = 0$, and $|h^z| < \frac{1}{4}$. And for slightly different initial product states, ballistic behavior was observed [40,41] also for $\gamma = w = \Delta = D^z = h^z = 0$, for which the model is integrable as well. *A priori* one would not expect ballistic spreading in generic models, but rather diffusive spreading. In Ref. [40], in particular, a preliminary analysis of the effect of some integrability-breaking perturbations pointed to a nonballistic spreading. In contrast, we find numerical evidence that ballistic behavior extends to a wide range of parameters, at least within the time window investigated.

V. MATERIALS AND METHODS

A. Simulations of the dynamics

Numerical simulations are performed with the Julia ITensor library [52]. We use a time-evolving block decimation (TEBD) algorithm, and, in all data reported, time evolution is discretized in time steps $\delta t = 0.01$ with second-order Trotter-Suzuki gates [53], using an MPS representation of the state with bond dimension up to 300 (see, e.g., [54]). We use finite-size chains with open boundary conditions. We always stop time evolution before the effects of the boundaries become

On the contrary, for the second class of perturbations, the probability distribution does not present two well-separated peaks, as shown, e.g., in the bottom row of Fig. 6. This rules out the formation of a cat state, but the basic features pointing to macroscopic entanglement (such as the linear growth in time of the difference of magnetization between flipping or not flipping the spin) are still present for times longer than our maximum simulation times.

relevant (such a time always exists because of Lieb-Robinson bounds). Being a product state, the initial state is conveniently represented also for very long chains, so the limitation to our simulations comes from time evolution: the growth of entanglement limits the size of $\Omega_\epsilon(t)$ that can be simulated. The largest $\Omega_\epsilon(t)$ that we have reached depends on the model considered and ranges from about 50 in the case of Fig. 4 to 130 in the case of Fig. 3.

B. Full counting statistics

The full probability distribution of a given observable encodes all the information about its moments. Let L be the chain length. We define $P_\theta(m)$ as the probability to get m from a measurement of $\mathbf{S}^z$ given that the system is in the state $|\Psi_\theta(t)\rangle$. Note that $m \in \{-\frac{L}{2}, -\frac{L}{2}+1, \ldots, \frac{L}{2}\}$. To set a convention, we assume L to be divisible by 4, so that the maximum possible value m of the magnetization is even. The generating function of the moments of the probability distribution is defined as

$$G_\theta(k) = \langle \Psi_\theta(t)| e^{i\frac{2\pi k}{L+1}\mathbf{S}^z} |\Psi_\theta(t)\rangle. \quad (14)$$

The probability $P_\theta(m)$ is then the Fourier transform of the generating function:

$$P_\theta(m) = \frac{1}{L+1} \sum_{k=-L/2}^{L/2} e^{-i\frac{2\pi k}{L+1}m} G_\theta(k). \quad (15)$$

We compute the generating function numerically using the Julia ITensor library [52].

We point out that, if the model is invariant under spin flip $\boldsymbol{\sigma}^{x,y} \to -\boldsymbol{\sigma}^{x,y}$, the state $|\Psi_{\pi/2}(t)\rangle$ belongs to the sector in which the parity operator $\mathbf{\Pi}^z = \prod_\ell \boldsymbol{\sigma}_\ell^z$ has eigenvalue -1, which means $P_{\pi/2}(m) = 0$ for any even m. This implies that, in the generic case of $|\Psi_\theta(t)\rangle$ with $\theta \neq \frac{\pi}{2}$, $P_\theta(m) = 0$ for any even m except for $P_\theta(L/2) = \cos^2 \theta$. For that reason, the plots of the probability distribution in models with spin-flip invariance show only $m = L/2$ and odd values of m.

C. Quantumness and quantum Fisher information

Reference [55] proposed to use the quantum Fisher information as a measure of the "macroscopicity" of quantum effects in lattice systems. The quantity of interest is, however, rather complicated to compute both analytically and numerically. Thus, for the sake of simplicity, we follow the approach of Refs. [27,28,56] and restrict ourselves to examining a sufficient condition. Specifically, we investigate the quantum Fisher information $\mathcal{F}(\mathbf{O})$ of extensive operators whose densities have support on a single site, i.e., $\mathbf{O}[\{\vec{n}\}] = \sum_{j \in \Omega_\epsilon(t)} \vec{n}_j \cdot \vec{\boldsymbol{\sigma}}_j$, where $\vec{\boldsymbol{\sigma}}_j \equiv \{\boldsymbol{\sigma}_j^x, \boldsymbol{\sigma}_j^y, \boldsymbol{\sigma}_j^z\}$ and the coefficients are normalized as $|\vec{n}_j|^2 = 1$. In pure states, which is the case we consider, $\mathcal{F}(\mathbf{O})$ equals four times the variance of $\mathbf{O}$. Using the notation of [29], we introduce the quantumness N_{eff} of a state as its maximal quantum Fisher information with respect to all extensive observables:

$$N_{\text{eff}} = \frac{1}{4|\Omega_\epsilon(t)|} \max_{\mathbf{O}} \mathcal{F}(\mathbf{O}). \quad (16)$$

We denote by $N_{\text{eff}}^{(1)}$ the maximization restricted to the observables with single-site density, as introduced above. N_{eff} was interpreted as an effective size of the macroscopic quantum state, thus $N_{\text{eff}}^{(1)}$ is a lower bound for the effective size.

In practice, we introduce the covariance matrix

$$[\text{K}(t)]_{n,\alpha;m,\beta} = \frac{1}{2} \langle \Psi_{\pi/2}(t)| \{\boldsymbol{\sigma}_n^\alpha, \boldsymbol{\sigma}_m^\beta\} |\Psi_{\pi/2}(t)\rangle$$
$$- \langle \Psi_{\pi/2}(t)|\boldsymbol{\sigma}_n^\alpha|\Psi_{\pi/2}(t)\rangle \langle \Psi_{\pi/2}(t)|\boldsymbol{\sigma}_m^\beta|\Psi_{\pi/2}(t)\rangle, \quad (17)$$

where $\{\boldsymbol{\sigma}_n^\alpha, \boldsymbol{\sigma}_m^\beta\} = \boldsymbol{\sigma}_n^\alpha \boldsymbol{\sigma}_m^\beta + \boldsymbol{\sigma}_m^\beta \boldsymbol{\sigma}_n^\alpha$. In pure states, $N_{\text{eff}}^{(1)}$ satisfies

$$N_{\text{eff}}^{(1)} = \frac{\text{tr}[\text{D}(t)]}{|\Omega_\epsilon(t)|} \quad \text{with} \quad \text{K}(t)\vec{v}(t) = [\text{D}(t) \otimes \text{I}_3]\vec{v}(t), \quad (18)$$

where $n, m \in \Omega_\epsilon(t)$ [the vector space is $3|\Omega_\epsilon(t)|$-dimensional] and $\text{D}(t)$ must be diagonal ($[\vec{v}]_n$ are normalized). We solve Eq. (18) using a Lanczos algorithm with three basic iterative steps:

(i) $\vec{w}^{(n)} = \text{K}\vec{v}^{(n)}$.
(ii) $[\text{D}^{(n)}]_j = \|\vec{w}_j^{(n)}\|^{-1}$.
(iii) $\vec{v}^{(n+1)} = (\text{D}^{(n)} \otimes \text{I}_3)\vec{w}^{(n)}$.

In all cases considered, this procedure worked well without the need for specific stabilizers.

VI. CONCLUSION

We have shown that macroscopic entanglement emerges from a localized perturbation in a low-entangled excited state in the middle of the spectrum, provided that such a stationary state does not maximize a local conservation law. In generic systems with local interactions, in particular, we observe the phenomenon in quantum scars with anomalously low bipartite entanglement. We further assert that in cases in which the excited state optimizes a semilocal conservation law, the macroscopic quantum state takes the simple form of a cat state. This, in turn, offers a novel approach to generating cat states within a subset of quantum many-body systems with local interactions.

This work leaves several open questions. First, a rigorous proof of the generation of cat states is missing. Second, the observation of ballistic behavior in generic systems could be questioned as a finite-time effect, so additional investigations are imperative. Third, we have only provided a preliminary and incomplete check of the stability of our protocol, but this is clearly an important issue and requires additional investigations.

APPENDIX A: ENERGY LEVEL STATISTICS

As a test of integrability or otherwise, we investigate the energy level statistics of the Hamiltonian of the spin-$\frac{1}{2}$

nearest-neighbor transistor chain,

$$\mathbf{H} = \sum_{\ell} \frac{1 - \sigma_{\ell}^z}{8} \left[J \vec{\sigma}_{\ell-1} \overset{S}{\cdot} \vec{\sigma}_{\ell+1} + \vec{D} \cdot (\vec{\sigma}_{\ell-1} \times \vec{\sigma}_{\ell+1}) \right]$$

$$- \frac{\vec{h}}{2} \cdot \vec{\sigma}_{\ell}, \tag{A1}$$

where $\vec{a} \overset{S}{\cdot} \vec{b} = \vec{a} \cdot (S\vec{b})$ and

$$S = \begin{bmatrix} \frac{1+\gamma}{2} & w & 0 \\ w & \frac{1-\gamma}{2} & 0 \\ 0 & 0 & \Delta \end{bmatrix}, \quad \vec{D} = \begin{bmatrix} 0 \\ 0 \\ D^z \end{bmatrix}, \quad \vec{h} = \begin{bmatrix} 0 \\ 0 \\ h^z \end{bmatrix}. \tag{A2}$$

We enforce periodic boundary conditions and restrict ourselves to the sector characterized by zero momentum, zero semilocal charge $\tilde{\mathbf{S}}^z$ (the largest eigenspace), and $\prod_j \sigma_j^z = \prod_j \sigma_{2j}^z = 1$.

Such a sector is equivalent to the sector with zero momentum, zero magnetization, and $\prod_j \tau_j^x = \prod_j \tau_j^z = 1$, of the Hamiltonian

$$\mathbf{H}_\tau = \sum_{\ell} J \frac{(1+\gamma)\mathbf{I} + (1-\gamma)\tau_{\ell-1}^z \tau_{\ell+2}^z}{4} \frac{\tau_\ell^x \tau_{\ell+1}^x + \tau_\ell^y \tau_{\ell+1}^y}{4}$$

$$+ \frac{(D^z + Jw)\tau_{\ell+2}^z + (D^z - Jw)\tau_{\ell-1}^z}{2} \frac{\tau_\ell^x \tau_{\ell+1}^y - \tau_\ell^y \tau_{\ell+1}^x}{4}$$

$$- \frac{h^z}{2} \tau_\ell^z \tau_{\ell+1}^z \tag{A3}$$

with periodic boundary conditions. Indeed, $\mathbf{H}_\tau$ is related to $\mathbf{H}$ by a Kramers-Wannier duality mapping, which transforms semilocal operators into odd local ones [30],

$$\sigma_j^x = \mathbf{\Pi}_{\tau,-}^x(j),$$

$$\sigma_j^y = \begin{cases} \tau_1^x \tau_2^z, & j = 1, \\ \mathbf{\Pi}_{\tau,-}^x(j-1)\tau_j^y \tau_{j+1}^z, & 1 < j < L, \\ -\tau_L^z, & j = L, \end{cases}$$

$$\sigma_j^z = \begin{cases} \tau_j^z \tau_{j+1}^z, & 1 \leqslant j < L, \\ \mathbf{\Pi}_\tau^x \tau_1^z \tau_L^z, & j = L, \end{cases} \tag{A4}$$
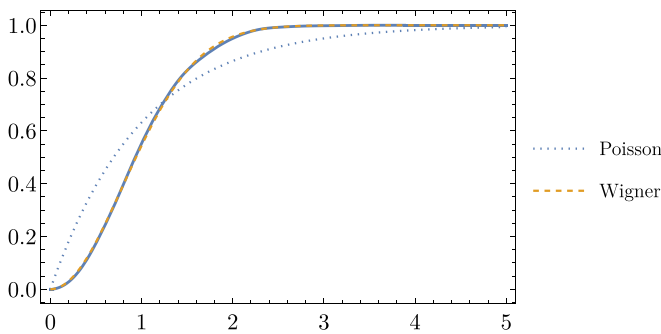

FIG. 7. Cumulative distribution of the unfolded energy level spacing in a sector of $\mathbf{H}$ with $J = 1$, $\gamma = 0.5$, $w = 0.7$, $\Delta = 0$, $D^z = 0.6$, $h^z = 0$ in a chain with 20 spins. The data are shown as a solid curve; the dotted and dashed curves are the (normalized) Poisson and Wigner-Dyson predictions expected in integrable and generic models, respectively.
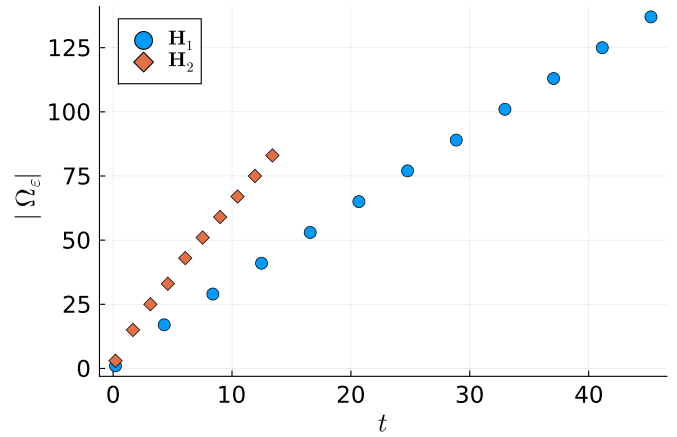

FIG. 8. Scaling in time of the effective system size for the models introduced in the main text. The accuracy ϵ is set to 0.001 and the parameters of $\mathbf{H}_1$ and $\mathbf{H}_2$ are those of Figs. 3 and 5, respectively.

where

$$\mathbf{\Pi}_{\tau,-}^x(j) = -\tau_1^y \prod_{\ell=2}^{j} \tau_\ell^x, \quad \mathbf{\Pi}_\tau^x = \prod_{\ell=1}^{L} \tau_\ell^x. \tag{A5}$$

Figure 7 shows quite clearly that the Hamiltonian of Fig. 3 in the main text is not integrable. Indeed, the cumulative distribution of the energy level spacing is in excellent agreement with the Wigner-Dyson distribution.

APPENDIX B: GROWTH OF THE EFFECTIVE SYSTEM $\Omega_\epsilon(t)$

The insets of Figs. 3–5 in the main text show that the effective system size, corresponding to the largest subsystem entangled with the rest, grows linearly in time. The dependency of $\Omega_\epsilon(t)$ on the time is explicitly shown in Fig. 8.
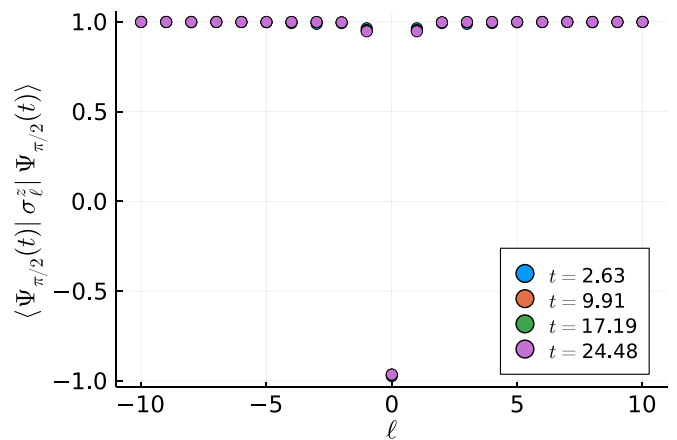

FIG. 9. Magnetization profile for the dual XXZ chain with $\mathcal{J} = 2.8$, $h^z = 1$. The magnetization does not change for any accessible time. The fact that the magnetization is maximal except for a few sites around the origin tells us that most of the system is in the $|\Uparrow\rangle$ state.

APPENDIX C: LOCALIZED EXCITATIONS

The main exception to the development of macroscopic entanglement after a local projective measurement is when the premeasurement state is the ground state in a disordered phase. We consider, for example, the dual XXZ Hamiltonian $\mathbf{H} = \mathcal{J}(\sum_\ell \sigma_{\ell-1}^x \frac{1-\sigma_\ell^z}{8} \sigma_{\ell+1}^x - \frac{h^z}{2}\sigma_\ell^z)$. If the intensity of the magnetic field $|h^z|$ is larger than $\frac{1}{2}$, the premeasurement state becomes the ground state, and a spin flip excites only local modes that do not spread with time—see Fig. 9.

APPENDIX D: ABSENCE OF MACROSCOPIC EFFECTS IN MODELS WITH U(1) SYMMETRY

In this Appendix, we prove that a state $|\Psi\rangle$ obtained by time evolution under a U(1)-symmetric Hamiltonian after a local perturbation to $|\Uparrow\rangle$ is macroscopically equivalent to $|\Uparrow\rangle$;

that is to say, the quantity $\langle\Psi|\mathbf{O}|\Psi\rangle - \langle\Uparrow|\mathbf{O}|\Uparrow\rangle$ is subextensive for any translational-invariant operator $\mathbf{O} = \sum_\ell \mathbf{O}_{A_\ell}$, with $\mathbf{O}_{A_\ell}$ local operators. We also prove that the variance of any of such operators $\mathbf{O}$ with respect to the state $|\Psi\rangle$ grows at most linearly with system $|\Omega_\epsilon(t)|$, ruling out the possibility to obtain a macroscopically entangled state from the time evolution of a locally perturbed $|\Uparrow\rangle$.

Let us denote by $|\Psi_s\rangle$ a state obtained by flipping s spins in $|\Uparrow\rangle$, or a linear combination of them. We start by observing that, if $\mathbf{S}^z$ is conserved, the state time-evolves as

$$|\Psi_s(t)\rangle = \sum_{n_1 < n_2 < \cdots < n_s} w_{\{n\}}(t)\sigma_{n_1}^- \sigma_{n_2}^- \cdots \sigma_{n_s}^- |\Uparrow\rangle$$

for some coefficients such that $\sum_{n_1 < n_2 < \cdots < n_s} |w_{\{n\}}|^2 = 1$. Let $\mathbf{O}_{A_\ell}$ be an operator with support in A, where A_ℓ is a set of $|A|$ adjacent sites starting with the ℓth spin: $A = \{\ell, \ldots, \ell + |A| - 1\}$. We have

$$
\langle\Psi_s(t)|\mathbf{O}_{A_\ell}|\Psi_s(t)\rangle - \langle\Uparrow|\mathbf{O}_{A_\ell}|\Uparrow\rangle
$$

$$
= \sum_{i=1}^s \sum_{\substack{n_1 < \cdots < n_s \\ n_k \in A_\ell \Leftrightarrow k=i}} \left(\sum_{\substack{n_i' \\ n_k' \in A_\ell, \forall k \in \{i\}}} w_{\{n\}}^*(t) w_{\{n\},n_i \to n_i'}(t) \langle\Uparrow|\sigma_{n_i'}^+ \mathbf{O}_{A_\ell} \sigma_{n_i}^-|\Uparrow\rangle - |w_{\{n\}}(t)|^2 \langle\Uparrow|\mathbf{O}_{A_\ell}|\Uparrow\rangle \right)
$$

$$
+ \sum_{i=1}^{s-1} \sum_{\substack{n_1 < \cdots < n_s \\ n_k \in A_\ell \Leftrightarrow k \in \{i,i+1\}}} \left(\sum_{\substack{n_i' < n_{i+1}' \\ n_k' \in A_\ell, \forall k \in \{i,i+1\}}} w_{\{n\}}^*(t) w_{\{n\},n_i \to n_i'}(t) \langle\Uparrow|\sigma_{n_i'}^+ \sigma_{n_{i+1}'}^+ \mathbf{O}_{A_\ell} \sigma_{n_i}^- \sigma_{n_{i+1}}^-|\Uparrow\rangle - |w_{\{n\}}(t)|^2 \langle\Uparrow|\mathbf{O}_{A_\ell}|\Uparrow\rangle \right)
$$

$$
+ \cdots + \sum_{\substack{n_1 < \cdots < n_s \\ n_k \in A_\ell, \forall k \in \{1,\ldots,s\}}} \left(\sum_{\substack{n_1' < \cdots < n_s' \\ n_k' \in A_\ell, \forall k \in \{1,\ldots,s\}}} w_{\{n\}}^*(t) w_{\{n'\}}(t) \langle\Uparrow|\sigma_{n_1'}^+ \cdots \sigma_{n_s'}^+ \mathbf{O}_{A_\ell} \sigma_{n_1}^- \cdots \sigma_{n_s}^-|\Uparrow\rangle - |w_{\{n\}}(t)|^2 \langle\Uparrow|\mathbf{O}_{A_\ell}|\Uparrow\rangle \right). \quad \text{(D1)}
$$

An upper bound for the absolute value of the left-hand side of the equation is obtained using $\langle v|\mathbf{O}|v\rangle \leqslant \|\mathbf{O}\| \langle v|v\rangle$, where $\|\mathbf{O}\|$ denotes the operator norm. Indeed, we have

$$
|\langle\Psi_s(t)|\mathbf{O}_{A_\ell}|\Psi_s(t)\rangle - \langle\Uparrow|\mathbf{O}_{A_\ell}|\Uparrow\rangle|
$$

$$
\leqslant 2\|\mathbf{O}_{A_\ell}\| \left(\sum_{i=1}^s \sum_{\substack{n_1 < \cdots < n_s \\ n_k \in A_\ell \Leftrightarrow k=i}} |w_{\{n\}}(t)|^2 + \sum_{i=1}^{s-1} \sum_{\substack{n_1 < \cdots < n_s \\ n_k \in A_\ell \Leftrightarrow k \in \{i,i+1\}}} |w_{\{n\}}(t)|^2 + \cdots + \sum_{\substack{n_1 < \cdots < n_s \\ n_k \in A_\ell, \forall k \in \{1,\ldots,s\}}} |w_{\{n\}}(t)|^2 \right)
$$

$$
\leqslant 2\|\mathbf{O}_{A_\ell}\| \sum_{i=1}^s \sum_{\substack{n_1 < \cdots < n_s \\ n_i \in A_\ell}} |w_{\{n\}}(t)|^2, \quad \text{(D2)}
$$

where the last step is not an equality because there are some coefficients w that are counted more than once in the last line (e.g., if we take $s = 2$ and $A_\ell = \{\ell, \ell + 1\}$, there is originally just one term $|w_{\ell,\ell+1}|^2$, coming from the sum $\sum_{\substack{n_1 < \cdots < n_s \\ n_k \in A_\ell, \forall k \in \{1,\ldots,s\}}}$, but the sum $\sum_{i=1}^s \sum_{\substack{n_1 < \cdots < n_s \\ n_i \in A_\ell}}$ has two such terms, which we get for $i = \ell$ and $i = \ell + 1$). Let us now consider the corresponding translational-invariant extensive operator $\mathbf{O} = \sum_{\ell \in \Omega_\epsilon(t)} \mathbf{O}_{A_\ell}$, where here Ω_ϵ has a generalized definition with respect to the main

text, since we want it to include all the light cones steaming from each spin flip. This gives

$$
\begin{aligned}
|\langle\Psi_s(t)|\mathbf{O}|\Psi_s(t)\rangle - \langle\Uparrow|\mathbf{O}|\Uparrow\rangle| &\leqslant \sum_{\ell\in\Omega_\epsilon(t)} |\langle\Psi_s(t)|\mathbf{O}_{A_\ell}|\Psi_s(t)\rangle - \langle\Uparrow|\mathbf{O}_{A_\ell}|\Uparrow\rangle| \\
&\leqslant 2\|\mathbf{O}_{A_1}\| \sum_{\ell\in\Omega_\epsilon(t)} \sum_{i=1}^{s} \sum_{\substack{n_1<\cdots<n_s \\ n_i\in A_\ell}} |w_{\{n\}}(t)|^2 \\
&\lesssim 2\|\mathbf{O}_{A_1}\|\,|A| \sum_{i=1}^{s} \sum_{n_1<\cdots<n_s} |w_{\{n\}}(t)|^2 = 2s\|\mathbf{O}_{A_1}\|\,|A|,
\end{aligned} \tag{D3}
$$

where we used translational invariance and $\lesssim$ rather than $\leqslant$ because $\Omega_\epsilon(t)$ is only approximately pure. This shows that $|\Psi_s(t)\rangle$ and $|\Uparrow\rangle$ are macroscopically indistinguishable for any time t.

We want now to extend the result to the square of the operator. We follow the same steps:

$$
\begin{aligned}
&\langle\Psi_s(t)|\mathbf{O}_{A_\ell}\mathbf{O}_{A_{\ell'}}|\Psi_s(t)\rangle - \langle\Uparrow|\mathbf{O}_{A_\ell}\mathbf{O}_{A_{\ell'}}|\Uparrow\rangle \\
&= \sum_{i=1}^{s} \sum_{\substack{n_1<\cdots<n_s \\ n_k\in A_\ell\cup A_{\ell'}\Leftrightarrow k=i}} \left(\sum_{\substack{n_i' \\ n_k'\in A_\ell\cup A_{\ell'},\forall k\in\{i\}}} w_{\{n\}}^*(t)w_{\{n\},n_i\to n_i'}(t)\langle\Uparrow|\sigma_{n_i'}^+\mathbf{O}_{A_\ell}\mathbf{O}_{A_{\ell'}}\sigma_{n_i}^-|\Uparrow\rangle - |w_{\{n\}}(t)|^2\langle\Uparrow|\mathbf{O}_{A_\ell}\mathbf{O}_{A_{\ell'}}|\Uparrow\rangle \right) \\
&\quad + \sum_{i<j=1}^{s} \sum_{\substack{n_1<\cdots<n_s \\ n_k\in A_\ell\cup A_{\ell'}\Leftrightarrow k\in\{i,j\}}} \left(\sum_{\substack{n_i'<n_j' \\ n_k'\in A_\ell\cup A_{\ell'},\forall k\in\{i,j\}}} w_{\{n\}}^*(t)w_{\{n\},\substack{n_i\to n_i' \\ n_j\to n_j'}}(t)\langle\Uparrow|\sigma_{n_i'}^+\sigma_{n_j'}^+\mathbf{O}_{A_\ell}\mathbf{O}_{A_{\ell'}}\sigma_{n_i}^-\sigma_{n_j}^-|\Uparrow\rangle - |w_{\{n\}}(t)|^2\langle\Uparrow|\mathbf{O}_{A_\ell}\mathbf{O}_{A_{\ell'}}|\Uparrow\rangle \right) \\
&\quad + \cdots + \sum_{\substack{n_1<\cdots<n_s \\ n_k\in A_\ell\cup A_{\ell'},\forall k\in\{1,\ldots,s\}}} \left(\sum_{\substack{n_1'<\cdots<n_s' \\ n_k'\in A_\ell\cup A_{\ell'},\forall k\in\{1,\ldots,s\}}} w_{\{n\}}^*(t)w_{\{n'\}}(t)\langle\Uparrow|\sigma_{n_1'}^+\cdots\sigma_{n_s'}^+\mathbf{O}_{A_\ell}\mathbf{O}_{A_{\ell'}}\sigma_{n_1}^-\cdots\sigma_{n_s}^-|\Uparrow\rangle \right. \\
&\qquad\qquad\qquad\left. - |w_{\{n\}}(t)|^2\langle\Uparrow|\mathbf{O}_{A_\ell}\mathbf{O}_{A_{\ell'}}|\Uparrow\rangle \right),
\end{aligned} \tag{D4}
$$

from which

$$
\begin{aligned}
|\langle\Psi_s(t)|\mathbf{O}_{A_\ell}\mathbf{O}_{A_{\ell'}}|\Psi_s(t)\rangle - \langle\Uparrow|\mathbf{O}_{A_\ell}\mathbf{O}_{A_{\ell'}}|\Uparrow\rangle| &\leqslant 2\|\mathbf{O}_{A_\ell}\|^2 \sum_{i=1}^{s} \sum_{\substack{n_1<\cdots<n_s \\ n_k\in A_\ell\cup A_{\ell'}\Leftrightarrow k=i}} |w_{\{n\}}(t)|^2 \\
&\quad + 2\|\mathbf{O}_{A_\ell}\|^2 \sum_{i<j=1}^{s} \sum_{\substack{n_1<\cdots<n_s \\ n_k\in A_\ell\cup A_{\ell'}\Leftrightarrow k\in\{i,j\}}} |w_{\{n\}}(t)|^2 + \cdots + 2\|\mathbf{O}_{A_\ell}\|^2 \sum_{\substack{n_1<\cdots<n_s \\ n_k\in A_\ell\cup A_{\ell'},\forall k\in\{1,\ldots,s\}}} |w_{\{n\}}(t)|^2 \\
&\leqslant 2\|\mathbf{O}_{A_\ell}\|^2 \sum_{i=1}^{s} \sum_{\substack{n_1<\cdots<n_s \\ n_i\in A_\ell\cup A_{\ell'}}} |w_{\{n\}}(t)|^2,
\end{aligned} \tag{D5}
$$

and finally

$$
\begin{aligned}
|\langle\Psi_s(t)|\mathbf{O}^2|\Psi_s(t)\rangle - \langle\Uparrow|\mathbf{O}^2|\Uparrow\rangle| &\leqslant \sum_{\ell,\ell'\in\Omega_\epsilon(t)} |\langle\Psi_s(t)|\mathbf{O}_{A_\ell}\mathbf{O}_{A_{\ell'}}|\Psi_s(t)\rangle - \langle\Uparrow|\mathbf{O}_{A_\ell}\mathbf{O}_{A_{\ell'}}|\Uparrow\rangle| \\
&\leqslant 2\|\mathbf{O}_{A_1}\|^2 \sum_{\ell,\ell'\in\Omega_\epsilon(t)} \sum_{i=1}^{s} \sum_{\substack{n_1<\cdots<n_s \\ n_i\in A_\ell\cup A_{\ell'}}} |w_{\{n\}}(t)|^2
\end{aligned}
$$

$$\leqslant 4 \| \mathbf{O}_{A_1} \|^2 \sum_{\ell, \ell' \in \Omega_\epsilon(t)} \sum_{i=1}^{s} \sum_{\substack{n_1 < \cdots < n_s \\ n_i \in A_\ell}} |w_{\{n\}}(t)|^2$$

$$\lesssim 4 \| \mathbf{O}_{A_1} \|^2 |A| |\Omega_\epsilon(t)| \sum_{i=1}^{s} \sum_{n_1 < \cdots < n_s} |w_{\{n\}}(t)|^2 = 4s \| \mathbf{O}_{A_1} \|^2 |A| |\Omega_\epsilon(t)|. \tag{D6}$$

This shows that the variance of any operator $\mathbf{O}$ on the state $|\Psi_s(t)\rangle$ coincides with the one on the state $|\Uparrow\rangle$ modulo corrections of order $O(|\Omega_\epsilon(t)|)$. Since $|\Uparrow\rangle$ is a state for which clustering of correlations holds and its variance cannot be larger than the system size, we obtain that the state $|\Psi_s(t)\rangle$ has the same properties, implying that it is not macroscopically entangled. Our proof can be easily generalized to any power of the operator, but higher powers are not needed for our purposes.

We now extend the results above to more general states. We consider first the quantity $\langle \Psi_{s'} | \mathbf{O} | \Psi_s \rangle$, $s \neq s'$, for two different states $|\Psi_s\rangle$ and $|\Psi_{s'}\rangle$. Without loss of generality, we can assume $s > s'$. We start from

$$|\langle \Psi_{s'} | \mathbf{O} | \Psi_s \rangle| \leqslant \sum_{\ell \in \Omega_\epsilon(t)} \sum_{n_1' < \cdots < n_{s'}'} \sum_{n_1 < \cdots < n_s} |\langle \Uparrow | \sigma_{n_1'}^+ \cdots \sigma_{n_{s'}'}^+ \mathbf{O}_{A_\ell} \sigma_{n_1}^- \cdots \sigma_{n_s}^- |\Uparrow\rangle| |w_{\{n'\}}'(t)| |w_{\{n\}}(t)|, \tag{D7}$$

and we rewrite the sums regrouping them, for fixed ℓ, according to how many of the primed indices $\{n'\}$ are outside the set A_ℓ. This is a number p that goes from 0 to s'. To get a nonzero contribution, the number of indices $\{n\}$ outside A_ℓ should also be p. The number of indices $\{n'\} \in A_\ell$ is then $s' - p \in \{0, \dots, s'\}$, while the number of indices $\{n\} \in A_\ell$ is $s - p \in \{s - s', \dots, s\}$; note that there is no contribution from $|A_\ell| < s - p$. For given p, there are $p + 1$ distinct subsets of consecutive n that can be in A_ℓ (they are characterized by the position of the first element of the subset); to keep track of this fact, we introduce a sum over an index j, such that the index n_j is the smallest of the indices $\{n\} \in A_\ell$. Such a decomposition leads to

$$|\langle \Psi_{s'} | \mathbf{O} | \Psi_s \rangle| \leqslant \sum_{\ell \in \Omega_\epsilon(t)} \sum_{p=0}^{s'} \sum_{j=1}^{p+1} \sum_{\substack{n_1 < \cdots < n_s \\ n_k \in A_\ell \Leftrightarrow j \leqslant k < j+s-p}}$$

$$\sum_{\substack{n_1' < \cdots < n_{s'-p}' \\ n_k' \in A_\ell, \forall k \in \{1, \dots, s'-p\}}} \left| \langle \Uparrow | \sigma_{n_1'}^+ \cdots \sigma_{n_{s'-p}'}^+ \mathbf{O}_{A_\ell} \sigma_{n_j}^- \cdots \sigma_{n_{j+s-p-1}}^- |\Uparrow\rangle \right| \left| w_{\{n\} \backslash \{n_j, \dots, n_{j+s-p-1}\} \cup \{n_1', \dots, n_{s'-p}'\}}'(t) \right| \left| w_{\{n\}}(t) \right|$$

$$\leqslant \| \mathbf{O}_{A_\ell} \| \sum_{p=0}^{s'} \sum_{j=1}^{p+1} \sum_{\ell \in \Omega_\epsilon(t)} \sum_{\substack{n_1 < \cdots < n_s \\ n_k \in A_\ell \Leftrightarrow j \leqslant k < j+s-p}} \sum_{\substack{n_1' < \cdots < n_{s'-p}' \\ n_k' \in A_\ell, \forall k \in \{1, \dots, s'-p\}}} \left| w_{\{n\} \backslash \{n_j, \dots, n_{j+s-p-1}\} \cup \{n_1', \dots, n_{s'-p}'\}}'(t) \right| \left| w_{\{n\}}(t) \right|. \tag{D8}$$

It is now convenient to write the sum over the indices n, n' in A_ℓ in another way. We introduce P_k^K as the set of all the k-tuples of increasing numbers in $\{0, \dots, K-1\}$. Note that P_k^K has $\binom{K}{k}$ elements. We then have

$$|\langle \Psi_{s'} | \mathbf{O} | \Psi_s \rangle| \leqslant \| \mathbf{O}_{A_\ell} \| \sum_{p=0}^{s'} \sum_{j=1}^{p+1} \sum_{\ell \in \Omega_\epsilon(t)} \sum_{(k_1, \dots, k_{s-p}) \in P_{s-p}^{|A|}} \sum_{(k_1', \dots, k_{s'-p}') \in P_{s'-p}^{|A|}}$$

$$\sum_{n_1 < \cdots < n_{j-1} < A_\ell < n_{j+s-p} < \cdots < n_s} \left| w_{\{n_1, \dots, n_{j-1}, \ell+k_1', \dots, \ell+k_{s'-p}', n_{j+s-p}, \dots, n_s\}}'(t) \right| \left| w_{\{n_1, \dots, n_{j-1}, \ell+k_1, \dots, \ell+k_{s-p}, n_{j+s-p}, \dots, n_s\}}(t) \right|, \tag{D9}$$

which we rewrite isolating the term with $p = s'$ (the case in which all the indices $\{n'\}$ are outside A_ℓ), which is special:

$$|\langle \Psi_{s'} | \mathbf{O} | \Psi_s \rangle| \leqslant \| \mathbf{O}_{A_\ell} \| \sum_{p=0}^{s'-1} \sum_{j=1}^{p+1} \sum_{(k_1, \dots, k_{s-p}) \in P_{s-p}^{|A|}} \sum_{(k_1', \dots, k_{s'-p}') \in P_{s'-p}^{|A|}} \sum_{\ell \in \Omega_\epsilon(t)}$$

$$\sum_{n_1 < \cdots < n_{j-1} < A_\ell < n_{j+s-p} < \cdots < n_s} \left| w_{\{n_1, \dots, n_{j-1}, \ell+k_1', \dots, \ell+k_{s'-p}', n_{j+s-p}, \dots, n_s\}}'(t) \right| \left| w_{\{n_1, \dots, n_{j-1}, \ell+k_1, \dots, \ell+k_{s-p}, n_{j+s-p}, \dots, n_s\}}(t) \right|$$

$$+ \| \mathbf{O}_{A_\ell} \| \sum_{j=1}^{s'+1} \sum_{(k_1, \dots, k_{s-s'}) \in P_{s-s'}^{|A|}} \sum_{\ell \in \Omega_\epsilon(t)}$$

$$\sum_{n_1 < \cdots < n_{j-1} < A_\ell < n_{j+s-s'} < \cdots < n_s} \left| w_{\{n_1, \dots, n_{j-1}, n_{j+s-s'}, \dots, n_s\}}'(t) \right| \left| w_{\{n_1, \dots, n_{j-1}, \ell+k_1, \dots, \ell+k_{s-s'}, n_{j+s-s'}, \dots, n_s\}}(t) \right|. \tag{D10}$$

Now, for fixed p, j, $\{k\}$, $\{k'\}$, we want to maximize the sums over ℓ, $\{n\}$ independently, which gives an upper bound to the full quantity. To that aim, we introduce the following compact notation: for the terms with $p < s'$,

$$\sum_{\ell \in \Omega_\epsilon(t)} \sum_{n_1 < \cdots < n_{j-1} < A_\ell < n_{j+s-p} < \cdots < n_s} \left| w'_{\{n_1,\ldots,n_{j-1},\ell+k'_1,\ldots,\ell+k'_{s'-p},n_{j+s-p},\ldots,n_s\}}(t) \right| \left| w_{\{n_1,\ldots,n_{j-1},\ell+k_1,\ldots,\ell+k_{s-p},n_{j+s-p},\ldots,n_s\}}(t) \right| \equiv \sum_{b \in B} W'_b W_b, \quad \text{(D11)}$$

and for the term $p = s'$,

$$\sum_{\ell \in \Omega_\epsilon(t)} \sum_{n_1 < \cdots < n_{j-1} < A_\ell < n_{j+s-s'} < \cdots < n_s} \left| w'_{\{n_1,\ldots,n_{j-1},n_{j+s-s'},\ldots,n_s\}}(t) \right| \left| w_{\{n_1,\ldots,n_{j-1},\ell+k_1,\ldots,\ell+k_{s-s'},n_{j+s-s'},\ldots,n_s\}}(t) \right| \equiv \sum_{\ell \in \Omega_\epsilon(t)} \sum_{c \in C} W'_c W_{c,\ell}, \quad \text{(D12)}$$

where b and c regroup all the indices that w and w' have in common, and W, W' are a synthetic expression for the coefficients that report only the indices we are interested in; note that in the first case, there are as many independent w as w', while for $p = s'$, w' does not depend on ℓ anymore. To maximize the expressions above, we should take into accounts the constraints $\sum_{n'_1 < \cdots < n'_{s'}} |w'_{\{n'\}}|^2 = 1$ and $\sum_{n_1 < \cdots < n_s} |w_{\{n\}}|^2 = 1$. In our search for the maximum, we can use the stronger conditions $\sum_{b \in B} W_b^2 = 1$ and $\sum_{b \in B} (W'_b)^2 = 1$ in the first case and $\sum_{c \in C} (W'_c)^2 = 1$ and $\sum_{c \in C, \ell \in \Omega_\epsilon(t)} W_{c,\ell}^2 = 1$ in the second case, which amount to requiring that the coefficients that are not involved in the sum are zero (given the original constraint, this maximizes the sum because all the terms are positive). Using the method of Lagrange multipliers, one can show that, under these constraints, $\sum_{b \in B} W'_b W_b$ is maximized by $W_b = W'_b$ and equals 1, while $\sum_{\ell \in \Omega_\epsilon(t)} \sum_{c \in C} W'_c W_{c,\ell}$ has degenerate points of maximum in $W_{c,\ell} = |\Omega_\epsilon(t)|^{-1/2} W'_c$ and gives $|\Omega_\epsilon(t)|^{1/2}$. In the end

$$|\langle \Psi_{s'} | \mathbf{O} | \Psi_s \rangle| \leqslant \|\mathbf{O}_{A_\ell}\| \sum_{j=1}^{s'+1} \sum_{(k_1,\ldots,k_{s-s'}) \in P^{|A|}_{s-s'}} |\Omega_\epsilon(t)|^{1/2} + O(|\Omega_\epsilon(t)|^0) = \|\mathbf{O}_{A_\ell}\| (s'+1) \binom{|A|}{s-s'} |\Omega_\epsilon(t)|^{1/2} + O(|\Omega_\epsilon(t)|^0).$$

$$\text{(D13)}$$

This result will be used below.

We finally consider a finite sum of states obtained by flipping different numbers of spins: $|\Psi^{(S)}\rangle = \sum_{s=1}^S a_s |\Psi_s\rangle$, where $a_j \in \mathbb{R}$, $\forall j$ (any potential phase can be absorbed in the states), and $\sum_{s=1}^S a_j^2 = 1$. From Eq. (D13) it readily follows that

$$|\langle \Psi_{S+1} | \mathbf{O} | \Psi^{(S)} \rangle| \leqslant \sum_{s=1}^S |\langle \Psi_{S+1} | \mathbf{O} | \Psi_s \rangle| \lesssim O(|\Omega_\epsilon(t)|^{1/2}). \quad \text{(D14)}$$

Let us now consider the state $|\Psi^{(2)}\rangle = a_1 |\Psi_1\rangle + a_2 |\Psi_2\rangle$, with $a_1, a_2 \in \mathbb{R}$ and $a_1^2 + a_2^2 = 1$. First of all, note that such a state is macroscopically equivalent to $|\Uparrow\rangle$. Indeed, using $\langle \Psi_2 | \mathbf{O} | \Psi_2 \rangle = \langle \Psi_1 | \mathbf{O} | \Psi_1 \rangle + O(|\Omega_\epsilon(t)|^0)$, which is a corollary of Eq. (D3), we have

$$\langle \Psi^{(2)} | \mathbf{O} | \Psi^{(2)} \rangle - \langle \Uparrow | \mathbf{O} | \Uparrow \rangle = a_1^2 \langle \Psi_1 | \mathbf{O} | \Psi_1 \rangle + a_2^2 \langle \Psi_2 | \mathbf{O} | \Psi_2 \rangle + 2a_1 a_2 \mathrm{Re}(\langle \Psi_1 | \mathbf{O} | \Psi_2 \rangle) - \langle \Uparrow | \mathbf{O} | \Uparrow \rangle$$

$$= 2a_1 a_2 \mathrm{Re}(\langle \Psi_1 | \mathbf{O} | \Psi_2 \rangle) + O(|\Omega_\epsilon(t)|^0) \lesssim O(|\Omega_\epsilon(t)|^{1/2}), \quad \text{(D15)}$$

which is subextensive. Similarly, we can conclude that $\langle \Psi^{(S)} | \mathbf{O} | \Psi^{(S)} \rangle - \langle \Uparrow | \mathbf{O} | \Uparrow \rangle \lesssim O(|\Omega_\epsilon(t)|^{1/2})$, meaning that $|\Psi^{(S)}\rangle$ is macroscopically equivalent to $|\Uparrow\rangle$ for any finite S. Let us now look at the variance of $\mathbf{O}$ in $|\Psi^{(2)}\rangle$:

$$\langle \Psi^{(2)}(t) | \mathbf{O}^2 | \Psi^{(2)}(t) \rangle - \langle \Psi^{(2)}(t) | \mathbf{O} | \Psi^{(2)}(t) \rangle^2 = a_1^2 \langle \Psi_1 | \mathbf{O}^2 | \Psi_1 \rangle + a_2^2 \langle \Psi_2 | \mathbf{O}^2 | \Psi_2 \rangle + 2a_1 a_2 \mathrm{Re}(\langle \Psi_1 | \mathbf{O}^2 | \Psi_2 \rangle)$$

$$- \left(a_1^2 \langle \Psi_1 | \mathbf{O} | \Psi_1 \rangle + a_2^2 \langle \Psi_2(t) | \mathbf{O} | \Psi_2(t) \rangle + 2a_1 a_2 \mathrm{Re}(\langle \Psi_1 | \mathbf{O} | \Psi_2(t) \rangle) \right)^2$$

$$= \langle \Psi_1 | \mathbf{O}^2 | \Psi_1 \rangle + 2a_1 a_2 \mathrm{Re}(\langle \Psi_1 | \mathbf{O}^2 | \Psi_2(t) \rangle) + O(|\Omega_\epsilon(t)|)$$

$$- (\langle \Psi_1 | \mathbf{O} | \Psi_1 \rangle + 2a_1 a_2 \mathrm{Re}(\langle \Psi_1 | \mathbf{O} | \Psi_2(t) \rangle) + O(|\Omega_\epsilon(t)|^0))^2, \quad \text{(D16)}$$

where we used $\langle \Psi_2 | \mathbf{O} | \Psi_2 \rangle = \langle \Psi_1 | \mathbf{O} | \Psi_1 \rangle + O(|\Omega_\epsilon(t)|^0)$ and $\langle \Psi_2 | \mathbf{O}^2 | \Psi_2 \rangle = \langle \Psi_1 | \mathbf{O}^2 | \Psi_1 \rangle + O(|\Omega_\epsilon(t)|)$ [corollaries of Eqs. (D3) and (D6)]. Using that the variance of any state $|\Psi_s\rangle$ cannot grow faster than $|\Omega_\epsilon(t)|$, we get

$$\langle \Psi^{(2)}(t) | \mathbf{O}^2 | \Psi^{(2)}(t) \rangle - \langle \Psi^{(2)}(t) | \mathbf{O} | \Psi^{(2)}(t) \rangle^2 = 2a_1 a_2 \left[\mathrm{Re}(\langle \Psi_1 | \mathbf{O}^2 | \Psi_2(t) \rangle) - \langle \Psi_1 | \mathbf{O} | \Psi_1 \rangle \mathrm{Re}(\langle \Psi_1 | \mathbf{O} | \Psi_2(t) \rangle) \right] + O(|\Omega_\epsilon(t)|).$$

$$\text{(D17)}$$

If the leading contribution to the variance were larger than $O(|\Omega_\epsilon(t)|)$, by changing the sign of a_1 we could make the variance negative; since the variance is by definition positive, by contradiction, we have that the leading order cannot be larger than $O(|\Omega_\epsilon(t)|)$. We can now assume that the variance in the state $|\Psi^{(S-1)}\rangle$ is of order $O(|\Omega_\epsilon(t)|)$ and show that this implies that the variance in $|\Psi^{(S)}\rangle$ is as well. The proof is essentially the same as above with just a small modification, namely

$\langle \Psi^{(S-1)}|\mathbf{O}|\Psi^{(S-1)}\rangle - \langle \Uparrow|\mathbf{O}|\Uparrow\rangle$ is $O(|\Omega_\epsilon(t)|^{1/2})$ rather than $O(|\Omega_\epsilon(t)|^{1/2})$. This gives an extra term in the potential leading order, which, however, does not affect the final result: calling $|\Psi^{(S)}\rangle = a_1 |\Psi_S\rangle + a_2 |\Psi^{(S-1)}\rangle$, we have

$$
\begin{aligned}
\langle \Psi^{(S)}(t)|\mathbf{O}^2|\Psi^{(S)}(t)\rangle - \langle \Psi^{(S)}(t)|\mathbf{O}|\Psi^{(S)}(t)\rangle^2 &= a_1^2 \langle \Psi_S|\mathbf{O}^2|\Psi_S\rangle + a_2^2 \langle \Psi^{(S-1)}|\mathbf{O}^2|\Psi^{(S-1)}\rangle + 2a_1 a_2 \mathrm{Re}(\langle \Psi_S|\mathbf{O}^2|\Psi^{(S-1)}\rangle) \\
&\quad - \left[a_1^2 \langle \Psi_S|\mathbf{O}|\Psi_S\rangle + a_2^2 \langle \Psi^{(S-1)}(t)|\mathbf{O}|\Psi^{(S-1)}(t)\rangle + 2a_1 a_2 \mathrm{Re}(\langle \Psi_S|\mathbf{O}|\Psi^{(S-1)}(t)\rangle)\right]^2 \\
&= \langle \Psi_S|\mathbf{O}^2|\Psi_S\rangle + 2a_1 a_2 \mathrm{Re}(\langle \Psi_S|\mathbf{O}^2|\Psi^{(S-1)}(t)\rangle) + O(|\Omega_\epsilon(t)|) \\
&\quad - \left[\langle \Psi_S|\mathbf{O}|\Psi_S\rangle + 2a_1 a_2 \mathrm{Re}(\langle \Psi_S|\mathbf{O}|\Psi^{(S-1)}(t)\rangle) + O(a_1^0|\Omega_\epsilon(t)|^{1/2})\right]^2 \\
&\lesssim 2a_1 a_2 \big[\mathrm{Re}(\langle \Psi_S|\mathbf{O}^2|\Psi^{(S-1)}(t)\rangle) - \langle \Psi_S|\mathbf{O}|\Psi_S\rangle \, \mathrm{Re}\big(\langle \Psi_S|\mathbf{O}|\Psi^{(S-1)}(t)\rangle \\
&\quad + O(a_1^0|\Omega_\epsilon(t)|^{1/2})\big)\big] + O(|\Omega_\epsilon(t)|).
\end{aligned}
\tag{D18}
$$

Since a_1 appears linearly as in the case $S = 2$, we can use the same trick and we have by contradiction that the variance in $|\Psi^{(S)}\rangle$ cannot grow faster than the system size.

In conclusion, we have proved that the state obtained by any local perturbation of $|\Uparrow\rangle$ is macroscopically equivalent to $|\Uparrow\rangle$ and the variance of any operator in this state does not grow faster than the system size, where the system size is defined by $\Omega_\epsilon(t)$.

---

[1] E. Schrödinger, Die gegenwärtige Situation in der Quantenmechanik, Naturwissenschaften **23**, 807 (1935).

[2] J. D. Trimmer, The present situation in quantum mechanics: A translation of Schrödinger's "cat paradox" paper, Proc. Am. Philos. Soc. **124**, 323 (1980).

[3] D. M. Greenberger, M. A. Horne, and A. Zeilinger, *Going Beyond Bell's Theorem* (Springer Netherlands, Dordrecht, 1989), pp. 69–72.

[4] J. S. Bell, On the Einstein Podolsky Rosen paradox, Phys. Phys. Fiz. **1**, 195 (1964).

[5] G. S. Agarwal, R. R. Puri, and R. P. Singh, Atomic Schrödinger cat states, Phys. Rev. A **56**, 2249 (1997).

[6] D. Lombardo and J. Twamley, Deterministic creation of macroscopic cat states, Sci. Rep. **5**, 13884 (2015).

[7] C. Wang, Y. Y. Gao, P. Reinhold, R. W. Heeres, N. Ofek, K. Chou, C. Axline, M. Reagor, J. Blumoff, K. M. Sliwa, L. Frunzio, S. M. Girvin, L. Jiang, M. Mirrahimi, M. H. Devoret, and R. J. Schoelkopf, A Schrödinger cat living in two boxes, Science **352**, 1087 (2016).

[8] B. Hacker, S. Welte, S. Daiss, A. Shaukat, S. Ritter, L. Li, and G. Rempe, Deterministic creation of entangled atom–light Schrödinger-cat states, Nat. Photon. **13**, 110 (2019).

[9] B. Alexander, J. J. Bollinger, and H. Uys, Generating Greenberger-Horne-Zeilinger states with squeezing and postselection, Phys. Rev. A **101**, 062303 (2020).

[10] Y. Zhao, R. Zhang, W. Chen, X.-B. Wang, and J. Hu, Creation of Greenberger-Horne-Zeilinger states with thousands of atoms by entanglement amplification, npj Quantum Inf. **7**, 24 (2021).

[11] M. Cosacchi, T. Seidelmann, J. Wiercinski, M. Cygorek, A. Vagov, D. E. Reiter, and V. M. Axt, Schrödinger cat states in quantum-dot-cavity systems, Phys. Rev. Res. **3**, 023088 (2021).

[12] Z. Wang, Z. Bao, Y. Wu, Y. Li, W. Cai, W. Wang, Y. Ma, T. Cai, X. Han, J. Wang, Y. Song, L. Sun, H. Zhang, and L. Duan, A flying Schrödinger's cat in multipartite entangled states, Sci. Adv. **8**, eabn1778 (2022).

[13] T. Comparin, F. Mezzacapo, and T. Roscilde, Multipartite entangled states in dipolar quantum simulators, Phys. Rev. Lett. **129**, 150503 (2022).

[14] W.-B. Gao, C.-Y. Lu, X.-C. Yao, P. Xu, O. Gühne, A. Goebel, Y.-A. Chen, C.-Z. Peng, Z.-B. Chen, and J.-W. Pan, Experimental demonstration of a hyper-entangled ten-qubit Schrödinger cat state, Nat. Phys. **6**, 331 (2010).

[15] J. Etesse, M. Bouillard, B. Kanseri, and R. Tualle-Brouri, Experimental generation of squeezed cat states with an operation allowing iterative growth, Phys. Rev. Lett. **114**, 193602 (2015).

[16] A. Omran, H. Levine, A. Keesling, G. Semeghini, T. T. Wang, S. Ebadi, H. Bernien, A. S. Zibrov, H. Pichler, S. Choi, J. Cui, M. Rossignolo, P. Rembold, S. Montangero, T. Calarco, M. Endres, M. Greiner, V. Vuletic, and M. D. Lukin, Generation and manipulation of Schrödinger cat states in Rydberg atom arrays, Science **365**, 570 (2019).

[17] C. Song, K. Xu, H. Li, Y.-R. Zhang, X. Zhu, Q. Guo, Z. Wang, W. Ren, J. Hao, H. Feng, H. Fan, D. Zheng, D.-W. Wang, H. Wang, and S.-Y. Zhu, Generation of multicomponent atomic Schrödinger cat states of up to 20 qubits, Science **365**, 574 (2019).

[18] A. Shimizu and T. Miyadera, Stability of quantum states of finite macroscopic systems against classical noises, perturbations from environments, and local measurements, Phys. Rev. Lett. **89**, 270403 (2002).

[19] H. Bernien, S. Schwartz, A. Keesling, H. Levine, A. Omran, H. Pichler, S. Choi, A. S. Zibrov, M. Endres, M. Greiner, V. Vuletić, and M. D. Lukin, Probing many-body dynamics on a 51-atom quantum simulator, Nature (London) **551**, 579 (2017).

[20] C. J. Turner, A. A. Michailidis, D. A. Abanin, M. Serbyn, and Z. Papić, Weak ergodicity breaking from quantum many-body scars, Nat. Phys. **14**, 745 (2018).

[21] S. Moudgalya, B. A. Bernevig, and N. Regnault, Quantum many-body scars and Hilbert space fragmentation: A review of exact results, Rep. Prog. Phys. **85**, 086501 (2022).

[22] S. Dooley, Robust quantum sensing in strongly interacting systems with many-body scars, PRX Quantum **2**, 020330 (2021).

[23] P. Zhang, H. Dong, Y. Gao, L. Zhao, J. Hao, J.-Y. Desaules, Q. Guo, J. Chen, J. Deng, B. Liu, W. Ren, Y. Yao, X. Zhang, S. Xu, K. Wang, F. Jin, X. Zhu, B. Zhang, H. Li, C. Song, Z. Wang, F. Liu, Z. Papić, L. Ying, H. Wang, and Y.-C. Lai, Many-body

Hilbert space scarring on a superconducting processor, Nat. Phys. **19**, 120 (2022).

[24] J.-Y. Desaules, F. Pietracaprina, Z. Papić, J. Goold, and S. Pappalardi, Extensive multipartite entanglement from su(2) quantum many-body scars, Phys. Rev. Lett. **129**, 020601 (2022).

[25] E. H. Lieb and D. W. Robinson, The finite group velocity of quantum spin systems, Commun. Math. Phys. **28**, 251 (1972).

[26] T. Morimae, A. Sugita, and A. Shimizu, Macroscopic entanglement of many-magnon states, Phys. Rev. A **71**, 032317 (2005).

[27] P. Hyllus, W. Laskowski, R. Krischek, C. Schwemmer, W. Wieczorek, H. Weinfurter, L. Pezzé, and A. Smerzi, Fisher information and multiparticle entanglement, Phys. Rev. A **85**, 022321 (2012).

[28] G. Tóth, Multipartite entanglement and high-precision metrology, Phys. Rev. A **85**, 022322 (2012).

[29] F. Fröwis, P. Sekatski, W. Dür, N. Gisin, and N. Sangouard, Macroscopic quantum states: Measures, fragility, and implementations, Rev. Mod. Phys. **90**, 025004 (2018).

[30] M. Fagotti, Global quenches after localized perturbations, Phys. Rev. Lett. **128**, 110602 (2022).

[31] M. Fagotti, V. Marić, and L. Zadnik, Nonequilibrium symmetry-protected topological order: Emergence of semilocal Gibbs ensembles, Phys. Rev. B **109**, 115117 (2024).

[32] M. den Nijs and K. Rommelse, Preroughening transitions in crystal surfaces and valence-bond phases in quantum spin chains, Phys. Rev. B **40**, 4709 (1989).

[33] D. Pérez-García, M. M. Wolf, M. Sanz, F. Verstraete, and J. I. Cirac, String order and symmetries in quantum spin lattices, Phys. Rev. Lett. **100**, 167202 (2008).

[34] M. Endres, M. Cheneau, T. Fukuhara, C. Weitenberg, P. Schauß, C. Gross, L. Mazza, M. C. Bañuls, L. Pollet, I. Bloch, and S. Kuhr, Observation of correlated particle-hole pairs and string order in low-dimensional Mott insulators, Science **334**, 200 (2011).

[35] E. Ilievski, M. Medenjak, T. Prosen, and L. Zadnik, Quasilocal charges in integrable lattice systems, J. Stat. Mech. (2016) 064008.

[36] L. Zadnik and M. Fagotti, The folded spin-1/2 XXZ model: I. diagonalisation, jamming, and ground state properties, SciPost Phys. Core **4**, 010 (2021).

[37] B. Pozsgay, T. Gombor, and A. Hutsalyuk, Integrable hard-rod deformation of the Heisenberg spin chains, Phys. Rev. E **104**, 064124 (2021).

[38] R. Z. Bariev, Integrable spin chain with two- and three-particle interactions, J. Phys. A **24**, L549 (1991).

[39] L. Zadnik, K. Bidzhiev, and M. Fagotti, The folded spin-1/2 XXZ model: II. Thermodynamics and hydrodynamics

[40] K. Bidzhiev, M. Fagotti, and L. Zadnik, Macroscopic effects of localized measurements in jammed states of quantum spin chains, Phys. Rev. Lett. **128**, 130603 (2022).

[41] L. Zadnik, S. Bocini, K. Bidzhiev, and M. Fagotti, Measurement catastrophe and ballistic spread of charge density with vanishing current, J. Phys. A: Math. Theor. **55**, 474001 (2022).

[42] C. Monroe, W. C. Campbell, L.-M. Duan, Z.-X. Gong, A. V. Gorshkov, P. W. Hess, R. Islam, K. Kim, N. M. Linke, G. Pagano, P. Richerme, C. Senko, and N. Y. Yao, Programmable quantum simulations of spin systems with trapped ions, Rev. Mod. Phys. **93**, 025001 (2021).

[43] H.-J. Mikeska and A. K. Kolezhuk, *One-dimensional Magnetism* (Springer, Berlin, 2004), pp. 1–83.

[44] G. Müller and R. E. Shrock, Implications of direct-product ground states in the one-dimensional quantum XYZ and XY spin chains, Phys. Rev. B **32**, 5845 (1985).

[45] M. van Horssen, E. Levi, and J. P. Garrahan, Dynamics of many-body localization in a translation-invariant quantum glass model, Phys. Rev. B **92**, 100305(R) (2015).

[46] N. Pancotti, G. Giudice, J. I. Cirac, J. P. Garrahan, and M. C. Bañuls, Quantum east model: Localization, nonthermal eigenstates, and slow dynamics, Phys. Rev. X **10**, 021051 (2020).

[47] S. Bravyi, M. B. Hastings, and F. Verstraete, Lieb-Robinson bounds and the generation of correlations and topological quantum order, Phys. Rev. Lett. **97**, 050401 (2006).

[48] V. Marić and M. Fagotti, Universality in the tripartite information after global quenches, Phys. Rev. B **108**, L161116 (2023).

[49] V. Zauner, M. Ganahl, H. G. Evertz, and T. Nishino, Time evolution within a comoving window: scaling of signal fronts and magnetization plateaus after a local quench in quantum spin chains, J. Phys.: Condens. Matter **27**, 425602 (2015).

[50] V. Eisler and F. Maislinger, Front dynamics in the XY chain after local excitations, SciPost Phys. **8**, 037 (2020).

[51] J. Mossel and J.-S. Caux, Relaxation dynamics in the gapped XXZ spin-1/2 chain, New J. Phys. **12**, 055028 (2010).

[52] M. Fishman, S. R. White, and E. Miles Stoudenmire, The ITensor software library for tensor network calculations, SciPost Phys. Codebases, 4 (2022).

[53] N. Hatano and M. Suzuki, *Finding Exponential Product Formulas of Higher Orders* (Springer, Berlin, 2005), pp. 37–68.

[54] R. Orús, A practical introduction to tensor networks: Matrix product states and projected entangled pair states, Ann. Phys. **349**, 117 (2014).

[55] L. Pezzé and A. Smerzi, Entanglement, nonlinear dynamics, and the Heisenberg limit, Phys. Rev. Lett. **102**, 100401 (2009).

[56] F. Fröwis and W. Dür, Measures of macroscopicity for quantum spin systems, New J. Phys. **14**, 093039 (2012).